

國立交通大學  
光電工程研究所  
碩士論文

利用碎形動力學研究單一原子在  
光子晶體中的自發輻射

Fractal dynamics of the spontaneous emission of  
an atom in photonic crystals

研究生：蔡明容

指導教授：謝文峰 教授

程思誠 教授

中華民國九十六年六月

利用碎形動力學研究單一原子在光子晶體中的自發輻射

Fractal dynamics of the spontaneous emission of  
an atom in photonic crystals

研究生：蔡明容

Student: Ming-Rung Tsai

指導教授：謝文峰 教授

Advisor : Prof. Wen-Feng Hsieh

程思誠 教授

Prof. Szu-Cheng Cheng



A Dissertation

Submitted to Institute of Electro-Optical Engineering  
College of Electrical Engineering and Computer Science

National Chiao Tung University

In partial Fulfillment of the Requirements

for the Degree of

Master of Engineering

in

Electro-Optical Engineering

June 2007

Hsinchu, Taiwan, Republic of China

中華民國九十六年六月

# 利用碎形動力學研究單一原子在 光子晶體中的自發輻射

研究生：蔡明容

指導老師：謝文峰 教授  
程思誠 教授

國立交通大學光電工程研究所



原子在光子晶體中的自發輻射具有長時間記憶(long-time memory)的效應。因此利用記憶核心(memory kernel)我們可以了解原子在等向性(isotropic)及非等向性(anisotropic)光子晶體的自發輻射會導致碎形現象(fractal phenomenon)產生。此種現象我們可以利用碎形微積分(fractional calculus)來描述。所以當原子的躍遷頻率(transition frequency)落在光子晶體中的光能隙(photonic band-gap)外時，利用碎形微積分我們不會有多值解的問題，也不會有非物理的狀態出現，而這些問題是在之前的研究[Phy. Rev. A 50, 1764 (1994)]中所會遇到的。

以上所探討的原子在空間中視為一個點(point-like)，不過在實際的情況下，原子是具有尺寸的。因此在有尺寸的效應之下，需要考慮多極(multi-pole)的貢獻。所以我們利用具有尺寸的記憶核心來探討對原子自發輻射的影響，會發現其偶合常數(coupling constant)會改變。

# Fractional dynamics of the spontaneous emission of an atom in photonic crystals

Student: Ming-Rung Tsai

Advisor : Prof. Wen-Feng Hsieh  
Prof. Szu-Cheng Cheng

Institute of Electro-Optical Engineering  
College of Electrical Engineering and Computer Science  
National Chiao Tung University



## Abstract

We use memory kernel to study the spontaneous emission of an atom in a photonic crystal with the isotropic band and anisotropic band. Our studies show that the long-time memory of the spontaneous emission in the photonic crystal induces a fractal phenomenon. Therefore, the fractional calculus is a natural mathematics to describe the fractal phenomenon. When the atomic transition frequency lies within the allowed band, using the fractional calculus we show that there is no multiple-valued problem and no fractionalized steady-state inversion encountered in the previous studies [J. Mod. Opt. 41, 353 (1994)]. On the other hand.

We also consider an atom with finite size effect leading to multipole contributions and yield the memory kernel with the same form as a point-like atom. However, the memory kernel including finite-size effect has different coupling constant.

## 致謝

時間真的過的好快，想起認識這個實驗室是大三作專題的時候，一眨眼研究所就要畢業了。在這段期間最最感謝的就是可愛平易近人的謝文峰老師，他讓我知道老師跟學生之間的關係也可以這麼像朋友，一起聊天、講八卦，當然在學業跟研究上也是不厭其煩的尊尊教誨著。

再來要感謝黃志賢學長在研究上的指導；還有實驗室的學長們，松哥、黃董、維仁，你們讓我知道要成為材料組的大老都要有一定的份量；小豪和國峰，感謝你們在我做專題的時候就很照顧我；智章學長，你真的是一個很有耐心的人，我們家穎書多虧你這些日子的照顧；還有 Pochi 和信民學長，你們都是學佛的，希望你們有一天可以修成正果。再來就是實驗室一姐-晴如學姊，你讓我知道一個人可以吃很多還可以維持曼妙的身材。實驗室的學弟妹也是功不可沒，超級有活力的賴小妹妹，你讓我知道，我講話其實還滿小聲的，還有你聊天的功力真是無人能匹敵阿！還有阿佩，你真的是很單純、天真的一個女生。能夠有你們這麼可愛的學妹們，我真的很開心。接著是可愛的一群學弟們，陳憶文、陳厚仁，你們兩個真的是一群很乖巧的學弟。徐瑋哲，歌也唱的很好聽，卡丁車也玩的不錯；林易慶，聽說鋼琴彈的很好，有機會彈給我聽；李岳勳，感覺你以後可以當股市大亨，加油！特別感謝，程思誠老師和吳靜娜學姐在學術上的指導，使我受益良多。

接著我要感謝的是實驗室的同窗們，在這兩年的研究生涯中，真的很感謝可以遇到你們。陳穎屁，認識你也快要邁入第五年了，我相信我們之間應該盡在不言中吧，希望你永遠都可以這樣開開心心的。魅力王玫丹，這兩年多虧了你的照顧，讓我每天不愁吃穿，載我去看病、泡溫泉、吃大餐，還有不時拿零食給我吃，讓我體重真是居高不下阿！接下來的日子，還要一起相扶相持喔！小郭，感謝你碩一載我去學開車，雖然你常睡過頭，害我有好多堂課沒上到這。不過我覺得你真的是一個滿正直的人，不過有時候要多為自己想想比較好喔，不要每次都讓自己吃虧。輝鴻同學，不要每次都跟我買一樣的東西好嘛，連 burberry 都要跟我搶！希望你到台南可以當奇美一哥喔！阿徐，跟你同學快要五年了，竟然在近五個月才發現你真實的個性，真是隱藏的太好了，我想陳穎書應該是功不可沒，leader 到群創也要加油喔！還有超會打羽球的冬山河，你真的很可口，不…是很可愛、很善良，接下來的日子要跟小郭一起奮鬥一起扶持喔，you can do it!

真的很感謝能遇到實驗室的大家，讓我認識不同的人，經歷不同的事，使我的人生更加的豐富、精采。希望你們在往後的日子都可以很充實、很快樂，遇到任何困難都可以迎刃而解。最後要感謝我的父母，謝謝他們除了金錢上的支持，同時在我遇到困難、不順心的時候給我精神上最大的安慰，我愛你們。

2007年7月 于交大

# Content

Abstract (in Chinese).....	i
Abstract (in English).....	ii
Acknowledgements.....	iii
Contents.....	iv
List of Figures.....	vi
<b>Chapter 1 Introduction.....</b>	<b>1</b>
1-1 Background.....	1
1-2 Motivation.....	3
1-3 Organization of the thesis.....	4
<b>Chapter 2 Theory and Methodology.....</b>	<b>5</b>
2-1 Dynamics of the spontaneous emission.....	5
2-2 Fractional solution of spontaneous emission in isotropic model.....	9
2-2.1 Singular density of states.....	10
2-2.2 Smoothed density of states.....	16
2-3 Fractional solution of spontaneous emission in anisotropic model.....	18
2-4 Spontaneous emission of a finite-size atom.....	20
<b>Chapter 3 Simulation and Discussion.....</b>	<b>23</b>
3-1 Spontaneous emission of a point-like atom.....	23
3-1.1 Isotropic model.....	23
3-1.2 Anisotropic model.....	27

3-1.3 Summary.....	30
3-2 Spontaneous emission of a finite-size atom.....	30
<b>Chapter 4 Conclusion and Future work.....</b>	<b>36</b>
4-1 Conclusion.....	36
4-2 Future works.....	37
<b>Appendix A.....</b>	<b>39</b>
<b>Reference.....</b>	<b>45</b>



# List of Figures

<b>Fig. 2-1</b>	Schematic representation of a two-level atom with atomic transition frequency $\omega_{21}$ and the band structure of photonic crystals with band-edge frequency.....	<b>11</b>
<b>Fig. 3-1</b>	Atomic population on the excited atomic state, as a function of $\beta_{It}$ , for various values of the atomic detuning inside the band gap.....	<b>26</b>
<b>Fig. 3-2</b>	Atomic population on the excited atomic state, as a function of $\beta_{It}$ , for various values of the atomic detuning inside the band gap and at the band edge.....	<b>26</b>
<b>Fig. 3-3</b>	Atomic population on the excited atomic state, for $\Delta c/\beta_I = 0.3$ with $\varepsilon = 0$ , $\varepsilon = 10^{-5}$ and $\varepsilon = 10^{-3}$ .....	<b>27</b>
<b>Fig. 3-4</b>	Atomic population on the excited atomic state in allowed band, as a function of $\beta_{At}$ for various values of the atomic detuning.....	<b>29</b>
<b>Fig. 3-5</b>	Atomic population on the excited atomic state in the photonic band gap, as a function of $\beta_{At}$ for various values of the atomic detuning.....	<b>29</b>
<b>Fig. 3-6</b>	Atomic population on the excited atomic state as a function of $\beta_{Ft}$ for $\Delta c/\beta_F = -1$ with various values of a/d ratio.....	<b>32</b>



<b>Fig. 3-7</b>	Atomic population on the excited atomic state, as a function of $\beta_F t$ for $\Delta_c/\beta_F = -5$ with various values of $a/d$ ratio.....	<b>32</b>
<b>Fig. 3-8</b>	Schematic illustration of the enlarging electric field distribution associated with an atom in photonic crystal.....	<b>33</b>
<b>Fig. 3-9</b>	Atomic population on the excited atomic state, as a function of $\beta_F t$ , for $\Delta_c/\beta_F = 1$ with various values of ratio from $a/d = 1/2$ (red line) to $a/d = 1/10$ (magenta line) and without the finite-size effect (black line).....	<b>33</b>
<b>Fig. 3-10</b>	Atomic population on the excited atomic state as a function of $\beta_F t$ for $\Delta_c/\beta_F = 5$ with various values of $a/d$ ratio.....	<b>34</b>
<b>Fig. 3-11</b>	Atomic population on the excited atomic state, as a function of $\beta_F t$ for $\Delta_c/\beta_F = -0.01$ with various values of $a/d$ ratio.....	<b>34</b>
<b>Fig. 3-12</b>	Atomic population on the excited atomic state as a function of $\beta_F t$ for $\Delta_c/\beta_F = 0.01$ with various values of $a/d$ ratio.....	<b>35</b>

# Chapter 1 Introduction

## 1-1 Background

Spontaneous emission is a fundamental concept in atomic physics. A new generation of experiments reveals that spontaneous radiation from excited atoms can be greatly suppressed or enhanced by placing the atoms between mirrors or in cavities [1]. This modification of spontaneous emission arises from the fact that a dielectric cavity acts as a local resonance mode for electromagnetic wave propagation. There is a long lifetime for radiation injected into the cavity and a perfect isolation of electromagnetic modes is possible if a localized state of light can be formed. The extent of isolation of modes inside the resonator from modes outside is measured by the quality factor of the cavity. We will expect very different dynamical features of spontaneous emission decay of an atom in photonic crystals from that in a high-Q microcavity [2].

Photonic crystals (PhC) constitute a new class of dielectric materials, in which the basic electromagnetic interaction is controllably altered over certain frequency and length scales. In photonic crystals, the synergetic interplay between the microcavity resonances of individual dielectric particles and the Bragg scattering resonances of the dielectric array leads to the formation of a photonic band gap (PBG), a range of frequencies for which electromagnetic wave propagation is classically forbidden [3]. The presence of the photonic band gap in the dispersion relation of the electromagnetic field gives rise to new phenomena in quantum optics, including the inhibition of the spontaneous [4] and strong localization of light [5] leading to important technological applications. Therefore, when an atom with a resonant transition within the frequency gap is placed in the photonic

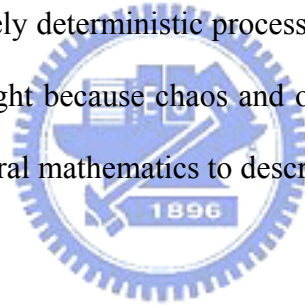
band-gap material, it has been predicted that the excited atom forms a photon-atom bound states [6], the optical analog of an electron-impurity level bound state in the gap of a semiconductor. The dispersion relation of photon is significantly modified near a photonic band edge, so the reservoir density of states becomes singular [7] and the atom-field interaction becomes strong when it becomes zero below the band-edge frequency.

More fundamentally, the correlation time of the electromagnetic vacuum fluctuation near a band edge is no longer negligibly small on the time scale of the evolution of an atomic system coupled to the electromagnetic (EM) field. In fact, the reservoir exhibits long-range temporal correlations, making the temporal distinction between atomic system and EM reservoir unclear. This renders the usual Born-Markov approximation [8] scheme invalid for the band gap systems. In such an interaction, the future of the atomic system is entirely determined by the present and not by the past. However, in the photonic crystal the Markov approximation that the spontaneous-emission atom loses all memory of its past is invalid and the atom-reservoir interaction becomes non-Markovian.

The time evolution of the probability amplitude of excited level of an atom is related to the delay Green function or memory kernel  $G(t-t')$  [7], which is a measure of the reservoir memory on the excited atom. The resultant Green function depends very strongly on the photon density of states of the relevant photon reservoir. In the free space, the density of field modes as a function of frequency is broad and slowly varying, resulting in a Green function (memory kernel) that exhibits Markovian behavior,  $G(t-t') = (\gamma/2) \delta(t-t')$ , where  $\gamma$  is the usual decay rate for spontaneous emission [9]. Studies of single atom spontaneous emission near a photonic band edge in the isotropic model [10,11] have shown that this non-Markovian system reservoir interaction gives rise to the time evolution

of the excited-state population such as decay and oscillatory behavior due to photon localization. The density of states in the isotropic model has the same square-root singularity-like has the form of  $\rho(\omega) \propto (\omega - \omega_c)^{-1/2}$ ,  $\omega > \omega_c$  and anisotropic model has the form of  $\rho(\omega) \propto (\omega - \omega_c)^{1/2}$ ,  $\omega > \omega_c$ . The memory kernel in the isotropic and anisotropic model have the forms  $G(\omega) \propto (t - t')^{-1/2}$ ,  $t > t'$  and  $G(\omega) \propto (t - t')^{1/2}$ ,  $t > t'$ , respectively.

Recently, the long-time memory phenomena have also attracted a great attention in statistical physics. There is no time scale to separate the microscopic levels from the macroscopic levels. Our studies show that the long-time memory of the spontaneous emission in the photonic crystal induces a fractal phenomenon. The fractional calculus provides a bridge between purely deterministic processes and purely stochastic ones. The fact is of interest in its own right because chaos and order in Nature coexist. Therefore, the fractional calculus is a natural mathematics to describe the fractal phenomenon.



## 1-2 Motivation

Of late, the long-time memory phenomena have also attracted a great attention in statistical physics. Such a long-time memory is intrinsic to all time scales of the phase space of a system, provided that the number of divisions generating a fractal set tends to infinity. The research of spontaneous emission of an atom in photonic crystals has been developed for a long time. However, using the Laplace transform method to solve the time evolution integral equation of the excited probability amplitude researched by John *et al.* [11], there is an unphysical state of fractionalized atomic population in the excited state when the resonant atomic frequency lies outside the band gap. In the thesis, we applied

the fractional calculus to study the dynamics of the spontaneous emission of an atom in photonic bandgap using singular and smoothed [12] density of states. In previous approach [11,12], the radiating atom is taken as a point-like electric dipole. Actually, a finite-size or an artificial atom and reservoir have stronger coupling, hence the finite-size effect and higher allowed multiple contributions can't be neglected. We will also use the density of states with finite-size effect [13] to calculate the memory kernel.

### **1-3 Organization of the thesis**

In this thesis, we divided the text into four chapters. We have narrated a brief statement of spontaneous emission to the background and our research motivations in this chapter. In Chapter 2, we apply the time-dependent Schrödinger equation to describe the spontaneous emission in vacuum field from a single atom and present the dynamics of spontaneous emission in photonic crystal with isotropic and anisotropic model. We also derive the population of spontaneous emission of an atom including finite-size effect. After that, we show our numerical results and discuss qualitatively possible processes in Chapter 3. In the end, the final conclusion and future works will be presented in Chapter 4.

## Chapter 2 Theory and Calculation Method

### 2-1 The dynamics of the spontaneous emission

In this section, we treat the atom-field interaction fully quantum mechanically, proving a basic understanding of spontaneous emission. It is well known that an atom in an excited state is not in a stationary state—it will eventually decay to the ground state by spontaneously emitting a photon. The nature of this evolution is due to the coupling of the atom to the electromagnetic vacuum field. Victor Weisskopf presented a method for analyzing this interesting problem in his thesis work, together with his advisor Eugene Wigner that is called *Weisskopf-Wigner theory* [14].

We begin by investigation a system involving the interaction of one two-level atom with all multi-modes field. Initially the atom is prepared in its excited state  $|2\rangle$  and the field is in vacuum state  $|\{0\}\rangle$ . We use

$$|\psi(0)\rangle = |2, \{0\}\rangle \quad (2.1)$$

to denote this initial state. Since this is not a stable state, the atom will decay to the ground  $|1\rangle$  state and give off a photon to one of the field modes  $(\mathbf{k},s)$ . These state vectors form a complete set for expanding the time-dependent state of the system:

$$|\psi(t)\rangle = A(t)e^{-i\omega_{21}t} |2, \{0\}\rangle + \sum_{\mathbf{k},s} B_{\mathbf{k}s}(t)e^{-i\omega_{\mathbf{k}s}t} |1, \{1_{\mathbf{k}s}\}\rangle, \quad (2.2)$$

where  $\omega_{21}$  is the atomic transition frequency and the initial condition is  $A(0)=1$ ,  $B_{\mathbf{k}s}(0)=0$ .

The state vector  $|2, \{0\}\rangle$  describes the atom in its excited state  $|2\rangle$  with no photons in

all reservoir modes, and the state vector  $|1, \{1_{ks}\}\rangle$  represents the atom in its ground state  $|1\rangle$  and a single photon in the mode with frequency  $\omega_{ks}$  with wavevector  $\mathbf{k}$  and polarization  $\mathbf{s}$ .

The total Hamiltonian for the coupled atom-reservoir system is  $H_{\text{tot}} = H_A + H_F + H_{\text{int}}$  (see appendix A).  $H_A$  represents the Hamiltonian of the free atom can be written as

$$H_A = \hbar\omega_{21}\sigma_{22}. \quad (2.3)$$

Here  $\sigma_{ij} = |i\rangle\langle j|$  ( $i, j = 1, 2$ ) are the atomic operators acting on level  $|j\rangle$  transforming it to level  $|i\rangle$  and  $\sigma_{ii} = |i\rangle\langle i|$  gives the population of level  $|i\rangle$ , that is, the probability to find the atom in level  $|i\rangle$ .  $H_F$  stands for the energy of the quantized radiation field in the absence of the atom (neglecting the zero-point energy). It is given by

$$H_F = \sum_{\mathbf{k}, \mathbf{s}} \hbar\omega_{ks} a_{ks}^\dagger a_{ks}, \quad (2.4)$$

where  $a_{ks}$  and  $a_{ks}^\dagger$  are the radiation field annihilation and creation operators with  $\mathbf{k}$  and  $\mathbf{s}$  ( $=1, 2$ ) representing, respectively. Let us now concentrate on the interaction Hamiltonian

$$H_{\text{int}} = -\hat{\mathbf{d}} \cdot \hat{\mathbf{E}}. \quad (2.5)$$

The dipole operator  $\hat{\mathbf{d}} = e\hat{\mathbf{r}}$  can be expressed as

$$\hat{\mathbf{d}} = \hat{\mathbf{d}}_{12}\hat{\sigma}_{12} + \hat{\mathbf{d}}_{21}\hat{\sigma}_{21}, \quad (2.6)$$

where we have used the property that states  $|1\rangle$  and  $|2\rangle$  have opposite parity such that

$\langle 1|\hat{\mathbf{r}}|1\rangle = \langle 2|\hat{\mathbf{r}}|2\rangle = 0$ . And the quantized electric field is [15]

$$\hat{E} = i \sum_{ks} \left[ \frac{\hbar \omega_{ks}}{2 \varepsilon_0 V} \right]^{1/2} \mathbf{e}_{ks} (a_{ks} e^{ik \cdot r} - a_{ks}^\dagger e^{-ik \cdot r}). \quad (2.7)$$

Here  $\mathbf{e}_{ks}$  is the unit vector of polarization for the reservoir mode  $(\mathbf{k}, \mathbf{s})$ , and  $\varepsilon_0$  is the permittivity of free space. In the optical regime of the spectrum where photon wavelengths are long compared to atomic dimensions ( $\lambda_{\text{photon}} \sim 10^3 \text{ \AA}$  and  $\lambda_{\text{atom}} \sim 1 \text{ \AA}$ ), it is useful to make the *electric dipole approximation* ( $\mathbf{k} \cdot \mathbf{r} \sim 0$ ) in Eq. (2.7). Thus the interaction Hamiltonian can be written as

$$H_{\text{int}} = i \hbar \sum_{k,s} g_{ks} (\sigma_{12} + \sigma_{21}) (a_{ks} - a_{ks}^\dagger), \quad (2.8)$$

where  $g_{\mathbf{k}}$  is the atom-field coupling constant

$$g_{\mathbf{k}} = \frac{\omega_{21} d_{21}}{\hbar} \left[ \frac{\hbar}{2 \varepsilon_0 \omega_{ks} V} \right]^{1/2} \mathbf{e}_{ks} \cdot \mathbf{u}_d. \quad (2.9)$$

Here  $d_{21}$  and  $\mathbf{u}_d$  are the absolute value and the unit vector of the atomic dipole moment,  $V$  is the sample volume. The interaction energy in Eq. (2.8) consists of four terms. The terms  $a_{ks}^\dagger \sigma_{12}$  describes the process in which the atom is taken from the upper state into the lower state and a photon of mode  $(\mathbf{k}, \mathbf{s})$  is created; the term  $a_{ks} \sigma_{21}$  describes the opposite process. The energy is conserved in both of the processes. The other two terms violate energy conservation, therefore we invoke the *rotation wave approximation* (RWA) to neglect the terms  $\sigma_{12} a_{ks}$  and  $\sigma_{21} a_{ks}^\dagger$ . The resulting simplified Hamiltonian is

$$H_{\text{int}} = i \hbar \sum_{k,s} g_{ks} (a_{ks}^\dagger \sigma_{12} - \sigma_{21} a_{ks}). \quad (2.10)$$

We want to determine the state of the atom and the state of the radiation field at some later time when the atom begins to emit photons and we do so in the



Weisskopf-Wigner approximation. From the Schrödinger equation

$$H|\psi(t)\rangle = i\hbar \frac{\partial}{\partial t} |\psi(t)\rangle, \quad (2.11)$$

we get the equations of motion for the probability amplitudes  $A(t)$  and  $B_{ks}(t)$  :

$$\frac{d}{dt} A(t) = -\sum_{k,s} g_{ks} B_{ks}(t) e^{-i\Omega_{ks}t}, \quad (2.12)$$

$$\frac{d}{dt} B_{ks}(t) = g_{ks} A(t) e^{i\Omega_{ks}t}. \quad (2.13)$$

where  $\Omega_{ks} = \omega_{ks} - \omega_{21}$  is the detuning frequency of the radiation frequency  $\omega_{ks}$  to the atomic transition frequency  $\omega_{21}$ . In order to get an equation that involves  $A(t)$  only, we first integrate Eq. (2.13).

$$B_{ks}(t) = g_{ks} \int_0^t A(t') e^{i\Omega_{ks}t'} dt'. \quad (2.14)$$

On substituting this expression of  $B_{ks}(t)$  into Eq. (2.12), we obtain

$$\frac{d}{dt} A(t) = -\sum_{k,s} |g_{ks}|^2 \int_0^t A(t') e^{-i\Omega_{ks}(t-t')} dt', \quad (2.15)$$

Thus,

$$\frac{d}{dt} A(t) = -\int_0^t G(t-t') A(t') dt', \quad (2.16)$$

where  $G(t-t')$  is the memory kernel (Green function), and is given by

$$G(t-t') = \sum_{k,s} |g_{ks}|^2 e^{-i\Omega_{ks}(t-t')}. \quad (2.17)$$

$G(t-t')$  is a measure of the reservoir's memory of its previous state on the time scale for the evolution of the probability amplitude of the system.

In free space, the density of the field modes is broad and slowly varying, resulting in a memory kernel that exhibits Markovian behavior,  $G(t-t') = (\gamma/2) \delta(t-t')$ , where  $\gamma$  is the usual decay rate for spontaneous emission [16]. In next section, we turn our attention to the case when the two-level atom is located within a photonic band structure, and assume photonic crystals are *absorptionless*. Using an effective-mass approximation to the full dispersion relation for a photonic crystal, we consider two models for the near-band-edge dispersion, isotropic and anisotropic model.

## 2-2 Fractional solution in isotropic model

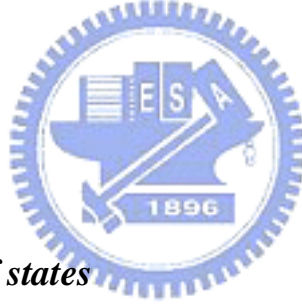
In the isotropic model of a photonic crystal, we assume that the Bragg condition is satisfied for the same wave vector magnitude for all directions in  $k$  space. Using an effective-mass approximation to the full dispersion relation for a photonic crystal, this gives a dispersion relation of the form  $\omega_k = \omega_c \pm A(|\vec{k}| - |\vec{k}_0|)^2$ . The positive (negative) sign indicates that  $\omega_k$  is expanded about the upper (lower) edge of the photonic band gap, and  $\omega_k$  is the frequency of the corresponding band edge. The bands above and below the gap can be distinguished by where the power of their modes lies – in the high- $\epsilon$  regions, or in the low- $\epsilon$  regions. Often the low- $\epsilon$  regions are air regions. For this reason, it is convenient to refer to the band above a photonic band gap as the “air band,” and the band below a gap as the “dielectric band.” It is a good approximation to completely neglect the effects of the lower photon bands by assuming the atom is located in the air regions [7]. Under these assumptions, the dispersion relation about the upper band (air band) edge is

$$\omega_k = \omega_c + A(|\vec{k}| - |\vec{k}_0|)^2, \quad (2.18)$$

where  $\omega_c$  is the bandedge frequency,  $\mathbf{k}_0$  is a point of the Brillouin zone boundary in the  $\mathbf{k}$  space instead of all direction, and  $A$  is a constant. The band-edge density of states generated by this dispersion relationship in the isotropic model has a singular form as

$$\rho(\omega) = \sum_{\mathbf{k}} \delta(\omega(\mathbf{k}) - \omega) \approx (\omega - \omega_c)^{-1/2}.$$

It is a fractal phenomenon that induces the long-time memory of the spontaneous emission in the photonic crystal. The natural mathematics of describing the fractal phenomenon is the fractional calculus. Using the fractional calculus we can evaluate derivatives and integrals with noninteger orders. Therefore, in next section we will treat the density of states in isotropic model as singularity and smoothing in isotropic model by applying fractional calculus to solve the time evolution integral equation of the excited probability amplitude.



### 2-2.1 Singular density of states

The band-edge density of states in the isotropic model has the singular form

$$\rho(\omega) = \sum_{\mathbf{k}} \delta(\omega(\mathbf{k}) - \omega) = \frac{\theta(\omega - \omega_c)}{\pi(\omega - \omega_c)^{1/2}} \quad (2.19)$$

where  $\theta$  is the step function. We change the  $\mathbf{k}$  summation to an integration by introducing a continuum density of states  $\rho(\omega)$  such that  $\rho(\omega)d\omega$  gives the number of oscillators in the frequency interval  $\omega$  to  $\omega+d\omega$  [17]. Hence we can obtain the memory kernel from Eq. (2.17) as

$$\begin{aligned}
G(t-t') &= \sum_{k,s} \int_0^{\infty} \rho(\omega) |g_{ks}|^2 e^{-i(\omega_{ks}-\omega_{21})(t-t')} d\omega \\
&= \beta_1^{3/2} \sqrt{\pi} \int_0^{\infty} \rho(\omega) e^{-i(\omega-\omega_{21})(t-t')} d\omega.
\end{aligned} \tag{2.20}$$

The memory kernel is obtained on substituting Eq. (2.19) into Eq. (2.20) and integrating over  $\omega$ , and the integral reduces to a complex Fresnel integral given by [18]

$$\int_0^{\infty} x^{p-1} e^{-\mu x} dx = \frac{1}{\mu^p} \Gamma(p), \tag{2.21}$$

where  $\Gamma$  is Gamma function and yields

$$G_1(t-t') = \beta_1^{3/2} \frac{e^{-i[\pi/4 - \Delta_c(t-t')]} }{\sqrt{t-t'}} \tag{2.22}$$

Here,  $\Delta_c = \omega_{21} - \omega_c$  is the detuning of the atomic resonant frequency from the band edge shown as in Fig. 2.1 and  $\beta_1^{3/2} = (\omega_{21}^2 d_{21}^2 k_0^2) / (12\pi^{3/2} \hbar \epsilon_0 \omega_c A^{1/2})$  is coupling constant.

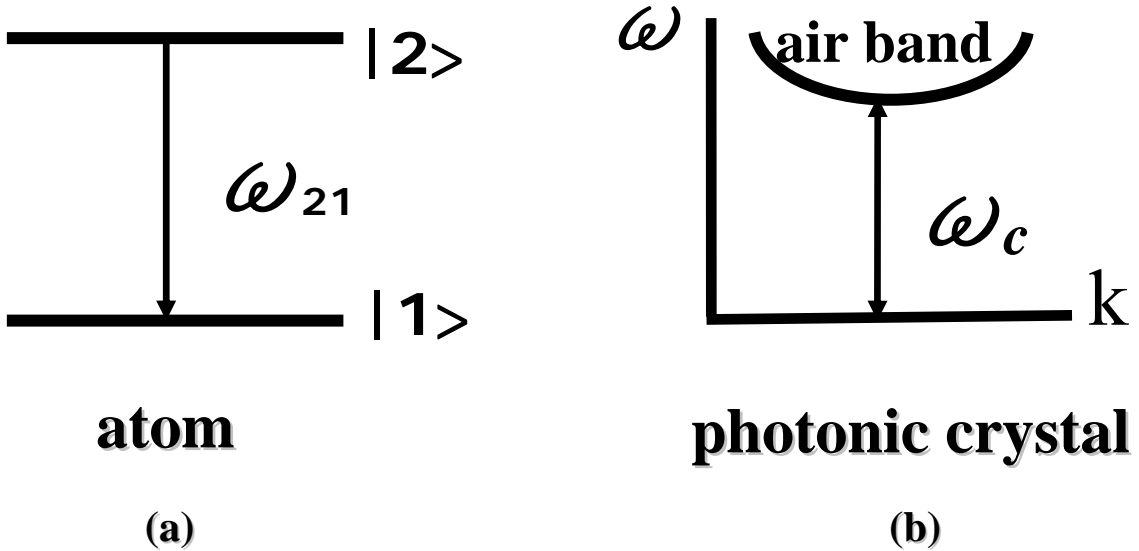


**Fig. 2-1.** (a) Schematic representation of a two-level atom with atomic transition frequency  $\omega_{21}$  and (b) the band structure of photonic crystals with band-edge frequency.

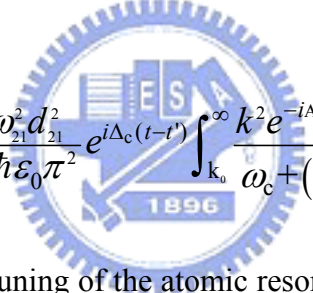
On the other hand, we can also replace the summation over  $\mathbf{k}$  by an integral:

$$\sum_{k,s} \rightarrow \sum_{s=1}^2 \int d^3k = 2 \frac{V}{(2\pi)^3} \int_0^\infty k^2 dk \int d\Omega, \quad (2.23)$$

where  $d^3\mathbf{k} \equiv k^2 dk d\Omega$ ,  $d\Omega$  being the solid angle element. Because the isotropic model associates the band edge with a sphere in  $k$  space, there is no angular dependence in the expansion of  $\omega_{\mathbf{k}}$  about the band edge. We may thus separate out the angular integration over solid angle  $\Omega$  in Eq. (2.17). Thus,  $G(t-t')$  can be expressed as

$$G(t-t') = \frac{\omega_{21}^2 d_{21}^2}{2\hbar \varepsilon_0} \frac{1}{(2\pi)^3} \frac{8\pi}{3} \int_0^\infty \frac{k^2 e^{-i(\omega_k - \omega_{21})(t-t')}}{\omega_k} dk. \quad (2.24)$$

Using isotropic dispersion relation near the upper band edge,  $\omega_{\mathbf{k}} = \omega_c + A(|\mathbf{k}| - |\mathbf{k}_0|)^2$ , Eq. (2.24) can be expressed as



$$G_1(t-t') = \frac{\omega_{21}^2 d_{21}^2}{6\hbar \varepsilon_0 \pi^2} e^{i\Delta_c(t-t')} \int_{k_0}^\infty \frac{k^2 e^{-iA(|k| - |k_0|)^2(t-t')}}{\omega_c + (|k| - |k_0|)^2} dk. \quad (2.25)$$

Here,  $\Delta_c = \omega_{21} - \omega_c$  is the detuning of the atomic resonant frequency from the band edge. For sufficiently large time, the integrand is a rapidly oscillating function of  $k$ . Thus the main contribution to the integral comes from the stationary point, that is,  $\mathbf{k} = \mathbf{k}_0$ . We can take  $k^2/\omega_{\mathbf{k}}$  in the integrand as  $k_0^2/\omega_c$ , hence the resulting integral is

$$G_1(t-t') = \frac{\omega_{21}^2 d_{21}^2}{6\hbar \varepsilon_0 \pi^2} e^{i\Delta_c(t-t')} \frac{k_0^2}{\omega_c} \int_{k_0}^\infty e^{-iA(|k| - |k_0|)^2(t-t')} dk. \quad (2.26)$$

We apply a complex Fresnel integral [18]

$$\int_0^\infty e^{-\mu^2 x^2} dx = \frac{\sqrt{\pi}}{2\mu} \quad (2.27)$$

in Eq. (2.26) to obtain the memory kernel

$$G_1(t-t') = \beta_1^{3/2} \frac{e^{-i[\pi/4 - \Delta_c(t-t')]} }{\sqrt{t-t'}}, \quad (2.28)$$

which is identical to Eq. (2.22).

Using the fractional calculus and making a transformation,  $A(t) = e^{i\Delta_c t} C(t)$ , Eq. (2.16) with memory kernel of Eq. (2.28) becomes

$$\frac{d}{dt} C(t) + i\Delta_c C(t) = -\beta_1^{3/2} e^{-i\pi/4} \int_0^t \frac{C(\tau)}{(t-\tau)^{1/2}} d\tau. \quad (2.29)$$

From the Riemann-Liouville fractional differentiation operator [19] defined by the formula

$$\frac{d^\alpha}{dt^\alpha} u(t) = \frac{1}{\Gamma(-\alpha)} \int_0^t (t-s)^{-\alpha-1} u(s) ds, \quad (2.30)$$

where  $\Gamma(x)$  is a gamma function. Using a fractional differentiation equation [20] Eq.

(2.29) can be expressed as:

$$\frac{d}{dt} C(t) + i\Delta_c C(t) = -\beta_1^{3/2} e^{-i\pi/4} \Gamma(1/2) \frac{d^{-1/2}}{dt^{-1/2}} C(t). \quad (2.31)$$

We can apply the integral operator  $d^{-1}/dt^{-1}$  first with  $C(0)=1$ , and then the fractional differentiation operator  $d^{3/2}/dt^{3/2}$  to Eq. (2.31) to obtain a *fractional Langevin equation* of the spontaneous emission of an atom in a photonic band gap,

$$\frac{d^{3/2}}{dt^{3/2}} C(t) + i\Delta_c \frac{d^{1/2}}{dt^{1/2}} C(t) + \sqrt{\pi} \beta_1^{3/2} e^{-i\pi/4} C(t) = -\frac{1}{2\sqrt{\pi}} t^{-3/2}. \quad (2.32)$$

We can solve Eq. (2.32) using the Laplace transform of  $C(t)$ ,

$$\tilde{C}(s) = \mathcal{L}\{C(t)\} = \int_0^\infty e^{-st} C(t) dt, \quad (2.33)$$

then the inverse Laplace transform of  $\tilde{C}(s)$ ,

$$C(t) = \mathcal{L}^{-1}\{\tilde{C}(s)\} = \frac{1}{2\pi i} \int_{\varepsilon-i\infty}^{\varepsilon+i\infty} e^{st} \tilde{C}(s) ds, \quad (2.34)$$

where the real number  $\varepsilon$  is chosen so that  $s = \varepsilon$  lies on the right of all singularities (poles and branch points) of function  $\tilde{C}(s)$ . Using the formulas of the fractional Laplace transform [19]

$$\mathcal{L}(t^\mu) = \frac{\Gamma(\mu+1)}{s^{\mu+1}}, \quad (2.35)$$

$$\mathcal{L}\left\{\frac{d^\alpha}{dt^\alpha} C(t)\right\} = s^\alpha \tilde{C}(s), \quad (2.36)$$

the Laplace transform  $\tilde{C}(s)$  can be found from Eq. (2.32) as

$$\tilde{C}(s) = \frac{\sqrt{s}}{s^{3/2} + i\Delta_c s^{1/2} - (i\beta)^{3/2}}, \quad (2.37)$$

where  $\beta^{3/2} = \beta_1^{3/2} \sqrt{\pi}$ . Converting the variable as  $s^{1/2} = X$ , we can then rewrite Eq. (2.37) as a sum of *partial fractions*

$$\tilde{C}(X) = \frac{a_1}{(X - X_1)} + \frac{a_2}{(X - X_2)} + \frac{a_3}{(X - X_3)}. \quad (2.38)$$

Note that the parameters  $X_n$  ( $n=1,2,3$ ) of Eq. (2.38) are the roots of  $X^3 + i\Delta_c X - (i\beta)^{3/2} = 0$ , which are also expressed in [11] as

$$X_1 = \beta^{1/2}(\eta_+ + \eta_-)e^{i\pi/4}, \quad (2.39)$$

$$X_2 = \beta^{1/2}(\eta_+ e^{-i\pi/6} - \eta_- e^{i\pi/6})e^{-i\pi/4}, \quad (2.40)$$

$$X_3 = \beta^{1/2}(\eta_+ e^{i\pi/6} - \eta_- e^{-i\pi/6})e^{i3\pi/4}, \quad (2.41)$$

$$\eta_{\pm} = \left[ \frac{1}{2} \pm \frac{1}{2} \sqrt{\left( 1 + \frac{4}{27} \frac{\Delta_c^3}{\beta^3} \right)} \right]^{1/3}, \quad (2.42)$$

and the coefficients  $a_n$  ( $n=1,2,3$ ) of Eq. (2.38) are given by

$$a_n = \frac{X_n}{(X_n - X_j)(X_n - X_m)} \quad (n \neq j \neq m; n, j, m = 1, 2, 3). \quad (2.43)$$

From the formula of the inverse fractional Laplace transform [19]

$$\mathcal{L}^{-1} \left\{ \frac{1}{s^{1/2} - a} \right\} = E_t \left( -\frac{1}{2}, a^2 \right) + a e^{a^2 t}, \quad (2.44)$$

we can yield the inverse Laplace transform of Eq. (2.38)

$$C(t) = \sum_{n=1}^3 a_n \left[ E_t \left( -\frac{1}{2}, X_n^2 \right) + X_n e^{X_n^2 t} \right] \quad (2.45)$$

or

$$A(t) = e^{it\Delta_c} \sum_{n=1}^3 a_n \left[ E_t \left( -\frac{1}{2}, X_n^2 \right) + X_n e^{X_n^2 t} \right], \quad (2.46)$$

where  $E_t(\alpha, a)$  is the fractional exponential function of order  $\alpha$  and is defined as

$$E_t(\alpha, a) = t^\alpha \sum_{n=0}^{\infty} \frac{(at)^n}{\Gamma(\alpha + n + 1)}. \quad (2.47)$$

The time evolution of the probability amplitude  $A(t)$  of an excited atom can be written in terms of the error function

$$\text{Erf}(z) = \frac{2}{\sqrt{\pi}} \int_0^z e^{-y^2} dy, \quad (2.48)$$

which is related to the fractional exponential function



$$E_t\left(\frac{1}{2}, a\right) = a^{-1/2} e^{at} \operatorname{Erf}(\sqrt{at}) \quad (2.49)$$

and

$$E_t\left(-\frac{1}{2}, a\right) = a E_t\left(\frac{1}{2}, a\right) + \frac{t^{-1/2}}{\sqrt{\pi}}. \quad (2.50)$$

From Eqs. (2.49) and (2.50), Eq. (2.46) can be written as

$$A(t) = e^{it\Delta_c} \sum_{n=1}^3 a_n \left( X_n + Y_n \left( \operatorname{Erf} \left( \sqrt{X_n^2 t} \right) \right) \right) e^{X_n^2 t}, \quad (2.51)$$

where  $Y_n = \sqrt{X_n^2}$  ( $n = 1, 2, 3$ ).

## 2-2.2 Smoothed density of states

The density of states in the isotropic model with a weak singularity  $(\omega - \omega_c)^{-1/2}$  for  $\omega > \omega_c$  had been smoothed out [12] by introducing a “cut-off smoothing” parameter  $\varepsilon$ .

The smoothed density of states can be written as

$$\rho^S(\omega) \propto \lim_{\varepsilon \rightarrow 0} \frac{(\omega - \omega_c)^{1/2}}{(\omega - \omega_c + \varepsilon)} \theta(\omega - \omega_c). \quad (2.52)$$

Applying the same steps use fractional calculus as Eq. (2.31) to Eq. (2.37) to obtain the Laplace transform of the excited-state amplitude as in Eq. (46) of Ref. [12]

$$\tilde{C}^S(s) = \frac{\sqrt{s} + \sqrt{i\varepsilon}}{s^{3/2} + \sqrt{i\varepsilon}s + i\Delta_c s^{1/2} + (i\sqrt{i\varepsilon}\Delta_c - \beta^{3/2}i^{3/4})}. \quad (2.53)$$

Instead of using complicated integration in Ref. [11], we use the formula in Eq. (2.44) to take the inverse fractional Laplace transform of Eq. (2.53)

$$C^S(t) = \sum_{n=1}^3 a_n^S \left[ E_t\left(-\frac{1}{2}, (X_n^S)^2\right) + X_n^S e^{(X_n^S)^2 t} \right] \quad (2.54)$$

or

$$A^S(t) = e^{it\Delta_c} \sum_{n=1}^3 a_n^S \left[ E_t\left(-\frac{1}{2}, (X_n^S)^2\right) + X_n^S e^{(X_n^S)^2 t} \right]. \quad (2.55)$$

The parameters  $X_n^S$  of Eq. (35) are the roots of  $s^{3/2} + \sqrt{i\varepsilon}s + i\Delta_c s^{1/2} + (i\sqrt{i\varepsilon}\Delta_c - \beta^{3/2}i^{3/4}) = 0$

as

$$X_1^S = \beta^{1/2}(\eta_+^S + \eta_-^S) e^{i\pi/4} - \frac{\sqrt{i\varepsilon}}{3}, \quad (2.56)$$

$$X_2^S = \beta^{1/2}(\eta_+^S e^{-i\pi/6} - \eta_-^S e^{i\pi/6}) e^{-i\pi/4} - \frac{\sqrt{i\varepsilon}}{3}, \quad (2.57)$$

$$X_3^S = \beta^{1/2}(\eta_+^S e^{i\pi/6} - \eta_-^S e^{-i\pi/6}) e^{i3\pi/4} - \frac{\sqrt{i\varepsilon}}{3}, \quad (2.58)$$

$$\eta_{\pm}^S = \left[ \frac{\left(1 - \frac{2\Delta_c\sqrt{\varepsilon}}{3\beta^{3/2}} - \frac{2\varepsilon^{3/2}}{27\beta^{3/2}}\right) \pm \sqrt{\left(1 - \frac{2\Delta_c\sqrt{\varepsilon}}{3\beta^{3/2}} - \frac{2\varepsilon^{3/2}}{27\beta^{3/2}}\right)^2 + \frac{4}{27}\left(\frac{\Delta_c - \varepsilon/3}{\beta}\right)^3}}{2} \right]^{1/3}. \quad (2.59)$$

The coefficients  $a_n^S$  of Eq. (35) is given by

$$a_n^S = \frac{X_n^S}{(X_n^S - X_j^S)(X_n^S - X_m^S)} \quad (n \neq j \neq m; n, j, m = 1, 2, 3). \quad (2.60)$$

## 2-3 Fractional solution in anisotropic model

We consider now a more realistic model, in which the dispersion relation is anisotropic. In anisotropic dispersion models, we account for the fact that, as  $\mathbf{k}$  moves away from  $\mathbf{k}_0$ , both the direction and magnitude of the band-edge wave vector are modified, and use an effective-mass approximation to the full dispersion relation for a photonic crystal. This gives a dispersion relation about the upper band (air band) edge is

$$\omega_k = \omega_c + A(\bar{k} - \bar{k}_0)^2. \quad (2.61)$$

The anisotropic effective mass dispersion relation leads to a photonic density of states at a band edge  $\omega_c$  which behaves as  $\rho(\omega) \approx (\omega - \omega_c)^{1/2}$ ,  $\omega > \omega_c$ . For our purposes, we shall therefore assume that  $A$  is a scalar constant, a condition that is satisfied exactly for crystal geometries in which the band-edge wave vector possesses cubic symmetry within the Brillouin zone [6], and is otherwise a reasonable approximation for the dispersion near a band edge after averaging over all directions.

Using the anisotropic effective mass dispersion relation Eq. (2.61) in Eq. (2.24) and making the substitution  $\mathbf{q} = \mathbf{k} - \mathbf{k}_0$  (so that  $d^3q = q^2 dq d\Omega$ ) we can evaluate the corresponding memory kernel  $G_A(t-t')$  is expressed as

$$G_A(t-t') = \frac{\omega_{21}^2 d_{21}^2}{6\hbar \varepsilon_0 \pi^2} e^{i\Delta_c(t-t')} \int_0^\infty \frac{q^2 e^{-iAq^2(t-t')}}{\omega_c + Aq^2} dq. \quad (2.62)$$

For large  $t-t'$ , the integral in Eq. (2.62) is dominated by the stationary phase point  $q = 0$ . Thus, the integral can be approximated by putting  $q = 0$  in the denominator, and using the integral [18]

$$\int_0^{\infty} x^2 e^{-px^2} dx = \frac{\sqrt{\pi}}{4p^{3/2}} \quad (2.63)$$

to obtain

$$G_A(t-t') = \beta_3^{1/2} \frac{e^{-i[3\pi/4 - \Delta_c(t-t')]} }{(t-t')^{3/2}}, \quad (2.64)$$

where  $\beta_3^{1/2} = (\omega_{21}^2 d_{21}^2) / (24\pi^{3/2} A^{3/2} \hbar \varepsilon_0 \omega_c)$ . Making a transformation  $A(t) = e^{i\Delta_c t} C(t)$  and using the fractional calculus Eq. (2.64) becomes

$$\frac{d}{dt} C(t) + i\Delta_c C(t) = -\beta_3^{1/2} e^{-i3\pi/4} \int_0^t \frac{C(\tau)}{(t-\tau)^{3/2}} d\tau. \quad (2.65)$$

From Eq. (2.30), we can express Eq. (2.65) as a fractional differentiation equation

$$\frac{d}{dt} C(t) + i\Delta_c C(t) = -\beta_3^{1/2} e^{-i3\pi/4} \Gamma(-1/2) \frac{d^{1/2}}{dt^{1/2}} C(t). \quad (2.66)$$

We can apply Eq. (2.36) to obtain the Laplace transform  $\tilde{C}(s)$  from Eq. (2.66) as

$$\tilde{C}(s) = \frac{1}{s + 2\beta_3^{1/2} e^{i\pi/4} s^{1/2} + i\Delta_c}, \quad (2.67)$$

where  $\beta_A^{1/2} = \beta_3^{1/2} \sqrt{\pi}$  and  $e^{-i3\pi/4} = -e^{i\pi/4}$ . Applying the *partial fractions* as Eq. (2.38),

we can then rewrite Eq. (2.67) under  $X_1 \neq X_2$  as a sum of *partial fractions*

$$\tilde{C}(X) = \frac{1}{(X_1 - X_2)} \left( \frac{1}{X - X_1} - \frac{1}{X - X_2} \right). \quad (2.68)$$

The parameters  $X_n$  are the roots of  $X^2 + 2\beta_A^{1/2} e^{-\pi/4} X + i\Delta_c X = 0$  which are expressed as

$$X_1 = e^{i\pi/4} (-\beta_A^{1/2} + \sqrt{\beta_A^{1/2} - \Delta_c}), \quad (2.69)$$

$$X_2 = e^{i\pi/4} (-\beta_A^{1/2} - \sqrt{\beta_A^{1/2} - \Delta_c}). \quad (2.70)$$

Using the formula in Eq. (2.44) we can obtain the inverse Laplace transform of Eq. (2.67)

$$C_1(t) = E_t(-\frac{1}{2}, X_1^2) + X_1 e^{X_1^2 t} - E_t(-\frac{1}{2}, X_2^2) - X_1 e^{X_2^2 t}. \quad (2.71)$$

For degenerate root  $X_1 = X_2$  (i.e.,  $\Delta_c = \beta^{1/2}$ ), Eq. (2.67) can be written as

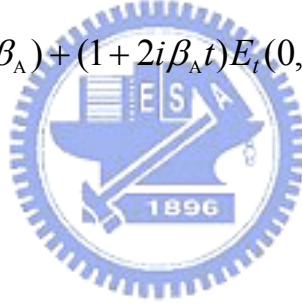
$$\tilde{C}(s) = \frac{1}{(s^{1/2} + \sqrt{i\beta_A})^2} \quad (2.72)$$

and from the formula [19]

$$\mathcal{L}^{-1} \left\{ \frac{1}{(s^{1/2} - a)^2} \right\} = 2atE_t(-\frac{1}{2}, a^2) + (1 + 2a^2t)E_t(0, a^2) + aE_t(\frac{1}{2}, a^2). \quad (2.73)$$

The inverse Laplace transform of Eq. (2.72) is given by

$$C_2(t) = -2\sqrt{i\beta_A}tE_t(-\frac{1}{2}, i\beta_A) + (1 + 2i\beta_A t)E_t(0, i\beta_A) - \sqrt{i\beta_A}E_t(\frac{1}{2}, i\beta_A). \quad (2.74)$$



## 2-4 Spontaneous emission of a finite-size atom

In our previous studies, the radiation atom is taken as a point-like electric dipole, neglecting its finite dimension as compared with the wavelength of the emitted light. However, for stronger coupling, as in the case of an atom with finite size may depend on the history of the spontaneous emission. Therefore, neglecting the finite atom-size effect and restriction to electric dipole transitions may become improper. In this section, we will carry out higher allowed multipole contributions.

In *dipole approximation*, the atom with an allowed transition is taken as a point-like electric dipole in the calculation of the correlation spectra, so that the factor  $e^{\mathbf{k} \cdot \mathbf{x}}$  is omitted.

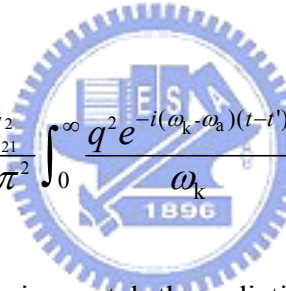
For such a point-like atom, the spectrum  $R_D(\omega)$  is

$$R_D(\omega) = \frac{\gamma_A \omega}{2\pi\omega_0}, \quad (2.75)$$

in which  $\gamma_A$  is the decay rate and  $\omega_0$  is the atomic transition frequency. On the other hand, the non-Markovian correlation spectra of spontaneous emission of an excited two-level atom are derived including the effect of finite size of the atom and all the possible contribution of allowed multipole radiations with the result [13]

$$R(\omega) = \frac{\gamma_A \omega}{2\pi\omega_0} \frac{1}{(1 + \omega^2 a^2 / c^2)^4}, \quad (2.76)$$

where the parameter  $a$  is particle size and  $c$  is light speed. Comparing Eq. (2.75) and Eq. (2.76), we can obtain the factor due to the finite size of the atom, which is  $1/(1 + \omega^2 a^2 / c^2)^4$ . Therefore, the memory kernel in Eq. (2.62) can be rewritten including the factor of finite-size effect as



$$G_F(t-t') = \frac{\omega_{21}^2 d_{21}^2}{6\hbar\epsilon_0\pi^2} \int_0^\infty \frac{q^2 e^{-i(\omega_k - \omega_a)(t-t')}}{\omega_k} \frac{1}{(1 + \omega_k^2 a^2 / c^2)^4} dq, \quad (2.77)$$

where  $\omega_k = \omega_c + Aq^2$ . In photonic crystal, the radiation wavelength is larger than particle size as  $\omega a / c \ll 1$  (i.e.,  $(1 + \omega_k^2 a^2 / c^2)^4 \approx 1 + 4\omega_k^2 a^2 / c^2$ ), thus Eq. (2.77) will reduce to

$$G_F(t-t') = \frac{\omega_{21}^2 d_{21}^2}{6\hbar\epsilon_0\pi^2} e^{i\Delta_c(t-t')} \int_0^\infty \frac{q^2 e^{-iAq^2(t-t')}}{\omega_c + Aq^2} \frac{1}{\left[1 + \frac{4a^2}{c^2} (\omega_c + Aq^2)^2\right]} dq. \quad (2.78)$$

For simplicity, we consider the spontaneous emission near photonic band edge, hence we have  $\omega_c \gg Aq^2$ , and Eq. (2.78) can be given by

$$G_F(t-t') = \frac{\omega_{21}^2 d_{21}^2}{6\hbar\epsilon_0\pi^2} e^{i\Delta_c(t-t')} \int_0^\infty \frac{q^2 e^{-iAq^2(t-t')}}{(\omega_c + p^2 \omega_c^3) + (3p^2 \omega_c^2 A + A)q^2} dq, \quad (2.79)$$

where  $p=2a/c$ . Applying Eq. (2.63) we can yield the same form as Eq. (2.64) with different coupling constant  $\beta_F$  as

$$G_A(t-t') = \beta_F^{1/2} \frac{e^{-i[3\pi/4 - \Delta_c(t-t')]} }{(t-t')^{3/2}}. \quad (2.80)$$

Comparing the coupling constant  $\beta_F$  and  $\beta_3$  as

$$\beta_F^{1/2} = \beta_3^{1/2} \frac{1}{(1+12a^2\omega_c^2/c^2)^{3/2}(1+4a^2\omega_c^2/c^2)}. \quad (2.81)$$

Applying the same step from Eq. (2.65) to Eq. (2.74) we can obtain the amplitude of excited state of spontaneous emission due to a finite size atom. In photonic crystal, the band-edge frequency can be approximated as  $\omega_c \approx 2c/d$  [21], here  $c$  is speed of light and  $d$  is the lattice constant for photonic crystals. Eq. (2.81) can be rewritten as

$$\beta_F^{1/2} = \beta_3^{1/2} \frac{1}{(1+48a^2/d^2)^{3/2}(1+16a^2/d^2)} \quad (2.82)$$

From Eq. (2.82), we can observe the coupling constant  $\beta_F$  is related to  $d$  (lattice constant) and  $a$  (particle size).

## Chapter 3 Numerical results and Discussion

### 3-1 Spontaneous emission of a point-like atom

#### 3-1.1 Isotropic model

As can be seen from Eq. (2.46), the dynamics of the spontaneous emission strongly depends on the detuning  $\Delta_c = \omega_{21} - \omega_c$ . Using the explicit form for  $A(t)$  in Eq. (2.46), we can calculate the probability  $P(t) = |A(t)|^2$  of the atom on the excited state in isotropic model and plot it on a time scale of the order of  $\beta$ .

Figure 3-1 shows the atomic population on the excited state as a function of the scaled time for various values of the atomic detuning *outside* the photonic band gap ( $\Delta_c > 0$ ). Outside the photonic band gap which means in the allowed band, the atomic population vanishes in the long-time limit, regardless how close the atomic frequency is to the band-edge frequency. In other words, the excited-state population eventually decays to zero (there is no population trapped on the upper level) due to the *propagating state* in the allowed band. The population decay becomes exponential for sufficiently large detuning into the allowed band, where the atom emits to the continuum modes with a decay rate proportional to the density of states. The closer photonic band edge, the density of states is bigger. Therefore, we can see that as increasing  $\Delta_c$  (the atomic level is resonant farther away from the band edge), the atom would decay very rapidly.

Figure 3-2 depicts the variation of  $\Delta_c$  with respect to the excited-state population *inside* the band gap ( $\Delta_c < 0$ ) and *at* the band edge ( $\Delta_c = 0$ ). We observe the excited-state population exhibits decay and oscillation behavior before reaching a nonzero steady-state



value due to photon localization. In other words, the spontaneously emitted photon will tunnel through the photonic crystal for a short length before being Bragg reflected back to the emitting atom to re-excite it. The result is a strongly coupled eigenstates of the electronic degrees of freedom of the atom and the electromagnetic modes of the dielectric. This is the *photon-atom bound state* and is the optical analogue of an electronic impurity level bound state in the gap of a semiconductor [22]. We note that the degree of localization of the upper state population for  $\omega_{21}$  within the gap is influenced by the density of states in the continuum of modes. This accounts for the absence of a completely localized state for  $\omega_{21}$  deep in the gap within our model.

Moreover, spontaneous emission in free space produces monotonic and irreversible decay of upper-level amplitude, whereas here we find the so-called *Rabi oscillation* and the generalized Rabi frequency is defined as  $\Omega_n = \sqrt{\Delta^2 + 4ng^2}$ , where  $\Delta$  is atomic detuning,  $n$  is the number of photons and  $g$  is coupling strength which is proportional to the overlap integral of the atom and the confined photon field. Hence, as  $|\Delta_c|$  is increased, the population oscillates faster due to the photon field being more confined, and reaches its steady-state value more quickly. We also find that there is no unphysical photon-atom bound state, as described in Refs. [11], in the allowed band.

For comparison, the probability  $P^S(t) = |A^S(t)|^2$  derived from the “cut-off smoothing” density of states in Eq. (2.55) for  $\Delta_c/\beta = 0.3$  (near-band edge condition) were plotted in Fig. 3-3 with  $\varepsilon = 0$  (i.e., the case of singular density of states as the solid curve),  $10^{-5}$  (dash curve), and  $10^{-3}$  (dot-dash curve), respectively. It also shows no unphysical photon-atom bound state with small oscillatory behavior in the short time regime and approaches zero in the long time limit. The probability  $P^S(t)$  of  $\varepsilon = 0$  is basically identical with that of  $\varepsilon = 10^{-5}$  and slightly differs for  $\varepsilon = 10^{-3}$ . Note that Fig. 3 of Ref. [12] was plotted for  $\Delta_c =$

$0.3\gamma_c = 0.3C\varepsilon^{-1/2} = 10\beta^{3/2}$ , which may be still far from the band edge in the allowed band, therefore, exhibits much faster decay. It is hard to tell whether the excited-state probability derived in [12] for the near bandedge ( $0 < \Delta_c < \beta$ ) would decay to zero in the long time limit or not.

By calculating the probabilities contributed from three  $X_n$ 's from Eq. (2.39) to Eq. (2.41) separately for  $\Delta_c/\beta = 0.01$ , we found these probabilities show decaying characteristics and only small oscillation in the short time regime even closer to the band edge. Indeed, it can be analytically shown that  $A(t)$  of Eq. (2.46) will always approach zero as  $t$  approaches infinity for positive detuning ( $\Delta_c > 0$ ) due to the first term,  $E_i(-\frac{1}{2}, X_n^2)$ , and the second term,  $X_n e^{X_n^2 t}$ , in the square bracket of Eq. (2.45) will asymptotically cancel out each other as  $t \rightarrow \infty$ . Thus, there is neither interference effect being involved in the decaying probability of the excited state nor photon-atom bound states existing near the allowed band. It might be that the photon will not strongly interact with atom in the allowed band. Therefore, in the allowed band, the atomic frequency shift may not provide enough strength to form the photon-atom bound state.

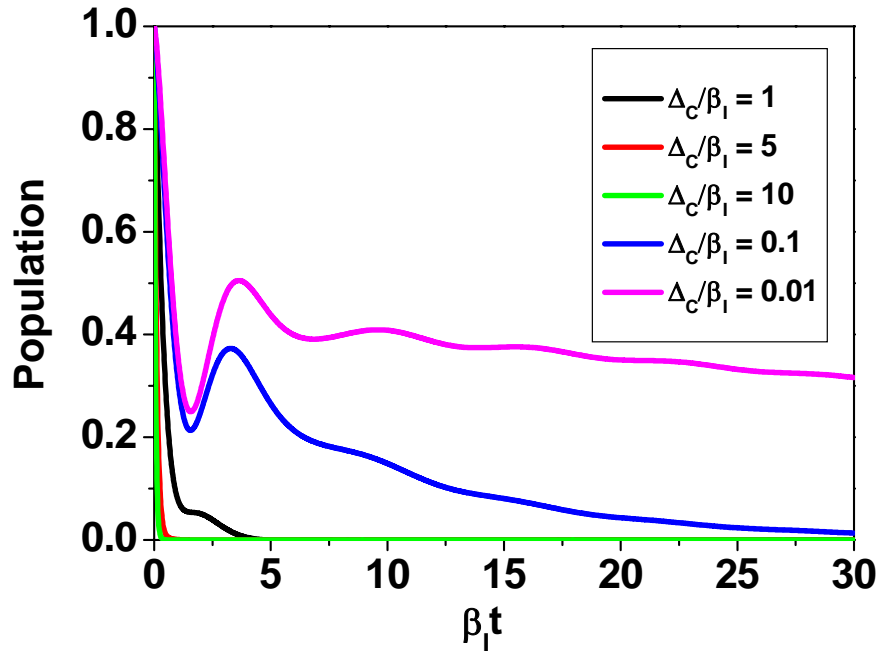


**Fig. 3-1.** Atomic population on the excited atomic state,  $P(t) = |A(t)|^2$ , as a function of  $\beta_1 t$ , for various values of the atomic detuning inside the band gap ( $\Delta_c/\beta_1 > 0$ ).

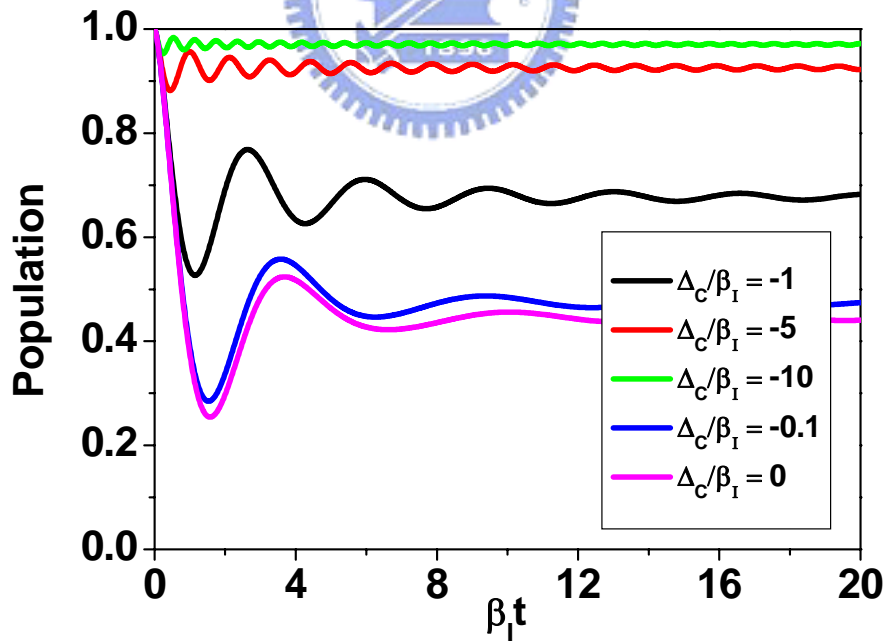


**Fig. 3-2.** Atomic population on the excited atomic state,  $P(t) = |A(t)|^2$ , as a function of  $\beta_1 t$ , for various values of the atomic detuning inside the band gap ( $\Delta_c/\beta_1 < 0$ ) and at the band edge ( $\Delta_c/\beta_1 = 0$ ).

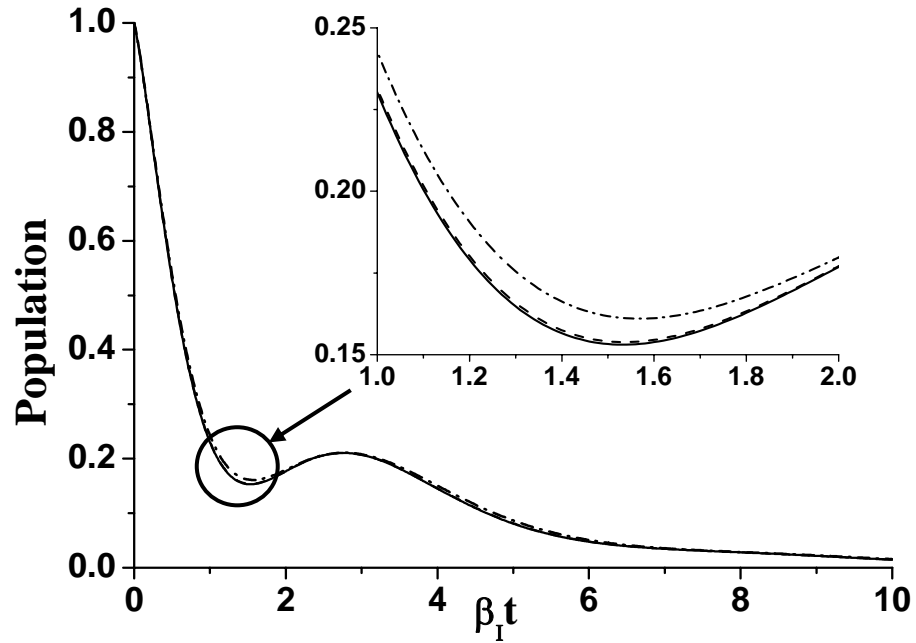
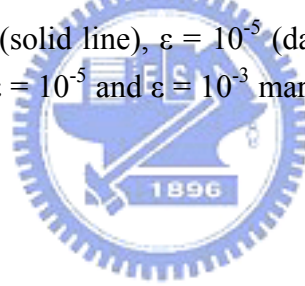


**Fig. 3-3.** Atomic population on the excited atomic state,  $P^S(t) = |A^S(t)|^2$  for  $\Delta_c/\beta_I = 0.3$  with three values of  $\varepsilon = 0$  (solid line),  $\varepsilon = 10^{-5}$  (dashed line) and  $\varepsilon = 10^{-3}$  (dot dashed line). The difference of  $\varepsilon = 0$ ,  $\varepsilon = 10^{-5}$  and  $\varepsilon = 10^{-3}$  marked by circle is enlarged and shown in the inset.



### 3-1.2 Anisotropic model

In anisotropic density of states, no singularity occurring like the isotropic density of states, the photon-atom bound states might also exist near the allowed band due to the shifted atomic frequency excitations. The temporal evolution of the excited atomic population for anisotropic model is given in Eqs. (2.71) and Eq. (2.74).

As shown in Fig. 3-4, when the atomic level is within the allowed band ( $\Delta_c > 0$ ), the propagating electromagnetic modes are present here. Hence, the atomic population vanishes in the long-time limit like in isotropic model. However, the population for  $\Delta_c = 0.01$  (blue line) and  $\Delta_c = 0.1$  (green line) decay faster in anisotropic model than in

isotropic model. This is because that the anisotropic model is more realistic causing imperfect localization.

Clearly, if the atomic level is inside the photonic band gap ( $\Delta_c < 0$ ) which is plotted in Fig. 3-5, the population also exhibits decay and oscillation behavior before reaching a nonzero steady-state value for  $\Delta_c/\beta_A = -1$  and  $\Delta_c/\beta_A = -5$  due to the number of stable localized states which is intimately connected to the behavior of the system in the long-time limit. One such state gives rise to a steady-state population in the excited level. These phenomena are the same as in the isotropic model except that the atomic population decay to zero for  $\Delta_c/\beta_A = -0.1$  and at band edge ( $\Delta_c/\beta_A = 0$ ). It is possible to realistically investigate the immediate neighborhood of the band-edge frequency in anisotropic model. When the atomic frequency is detuned into the band gap, a superposition of the continuum states and a bound state leads the emitted photon to the atom. Therefore, the atomic population again displays fractionalized inversion for relatively small values of the atomic detuning. However, this phenomenon should not be due to Lamb shift, which is only in order of  $10^{-7}$  [23], the Lamb shift may not provide enough strength to push the atomic frequency to the gap to form the photon-atom bound state.

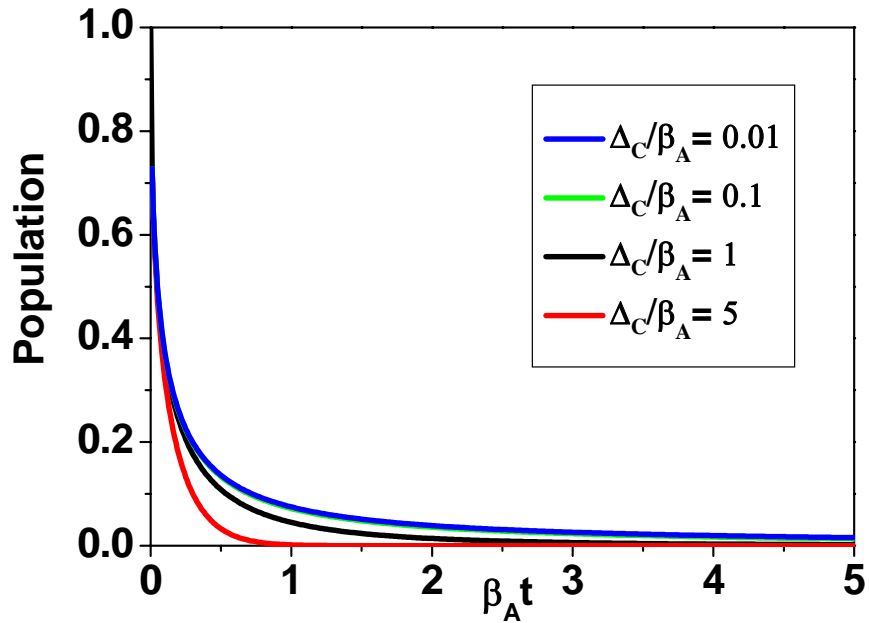


**Fig. 3-4.** Atomic population on the excited atomic state in allowed band,  $P(t) = |A(t)|^2$ , as a function of  $\beta_A t$ , for various values of the atomic detuning from  $\Delta_C/\beta_A = 0.01$  (blue line) to  $\Delta_C/\beta_A = 5$  (red line).

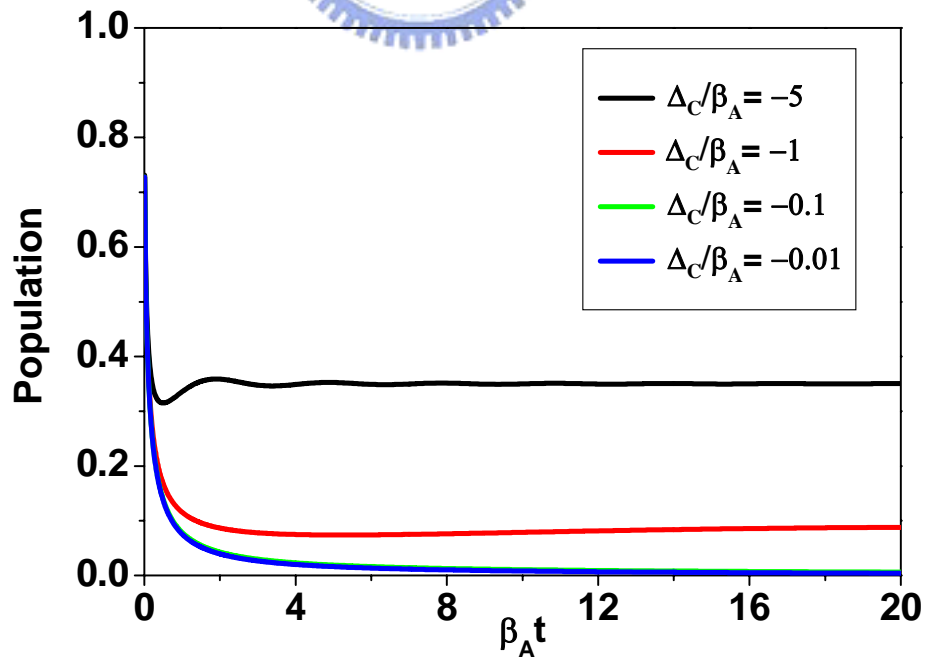


**Fig. 3-5.** Atomic population on the excited atomic state in the photonic band gap,  $P(t) = |A(t)|^2$ , as a function of  $\beta_A t$ , for various values of the atomic detuning from  $\Delta_C/\beta_A = -5$

(black line) to  $\Delta_c/\beta_A = -0.01$  (blue line).

### 3-1.3 Summary

In this section, we have reported the properties of spontaneous emission of an atom under dipole approximation in an isotropic and anisotropic model. We find a propagating state corresponding to transition frequency outside the photonic gap, therefore the population vanishes in the long-time limit in the isotropic and anisotropic model. On the other hand, the dressed state corresponding to transition frequency inside the gap is a non-decaying photon-atom bound state except that the atomic population decays to zero when the detuning frequency is close to photonic band-edge.



## 3-2 Spontaneous emission of a finite-size atom

From Eq. (2.82), we can obtain the relationship between the coupling constant  $\beta_F$  and the ratio of particle size to lattice constant ( $a/d$ ). In this section, we use various values of  $a/d$  to calculate the probability of the atom with finite-size effect.

In Fig. 3-6 and Fig. 3-7, we plot the population on the excited state with various values of ratio from  $a/d = 1/2$  to  $a/d = 1/50$  and without the finite-size effect ( $a = 0$ ) for  $\Delta_c/\beta_F < 0$  (in the band gap). We find that the excited-state population with finite-size effect exhibits decay and oscillatory behavior before reaching a nonzero steady-state which is bigger as the atom size increasing. These effects are due to the strong coupling between atom and field resulting in confinement which localizes photon like defect modes where the atom is present. As we known, the defect mode enhances electric field than the rest [24] shown in Fig. 3.8. This implies that by increasing the atom size, the

confinement becomes stronger. Accordingly, the generalized Rabi frequency mentioned above leads to the higher oscillatory frequency as increasing atom size due to the stronger coupling with the confined field or the larger  $g$ . The atomic population for  $\Delta/\beta_F = -1$  with  $a/d = 1/10$  is close to the population for  $\Delta/\beta_F = -5$  without the size effect, but their oscillatory frequencies are different. This is because the Rabi frequency is decided by both the detuning frequency and the coupling strength.

We plot the population within the allowed band and use various values of  $a/d$  for  $\Delta/\beta_F = 1$  and  $\Delta/\beta_F = 5$  in Figs. 3-9 and Fig. 3-10, respectively. The decay rate decreases as the size increasing is also due to the enhanced atom-filed coupling that induces the deeper defect potential or the larger defect dielectric constant. By comparison with Fig. 3-11 and Fig. 3.12, we can observe that the population is close with various values of ratio from  $a/d = 1/2$  to  $a/d = 1/10$ . The reason for this similarity is that when the atomic frequency is detuned near the band gap, a superposition of the continuum states and a bound state leads the emitted photon to the atom.



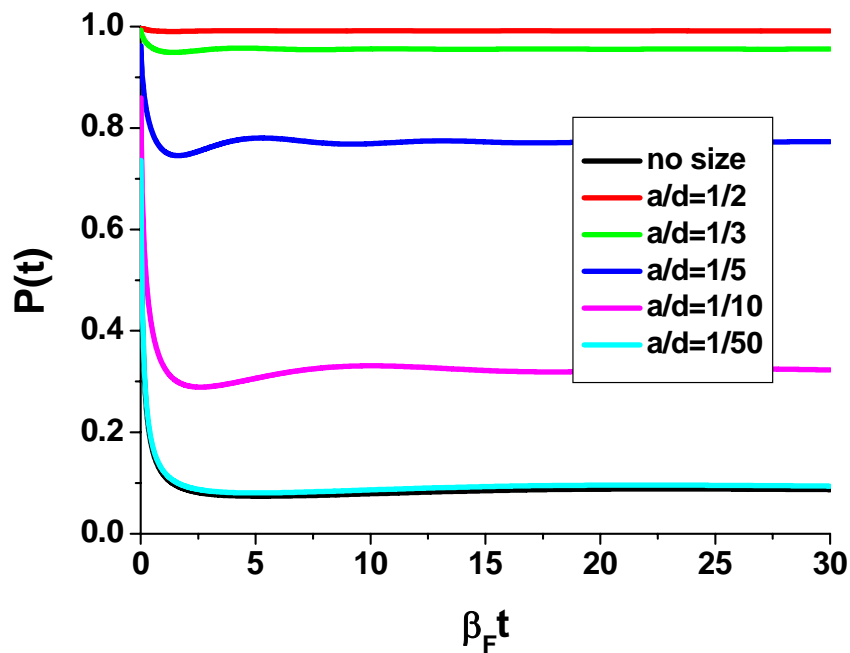


**Fig. 3-6.** Atomic population on the excited atomic state, as a function of  $\beta_F t$ , for  $\Delta/\omega_F = -1$  with various values of ratio from  $a/d = 1/2$  (red line) to  $a/d = 1/10$  (magenta line) and without the finite-size effect (black line).

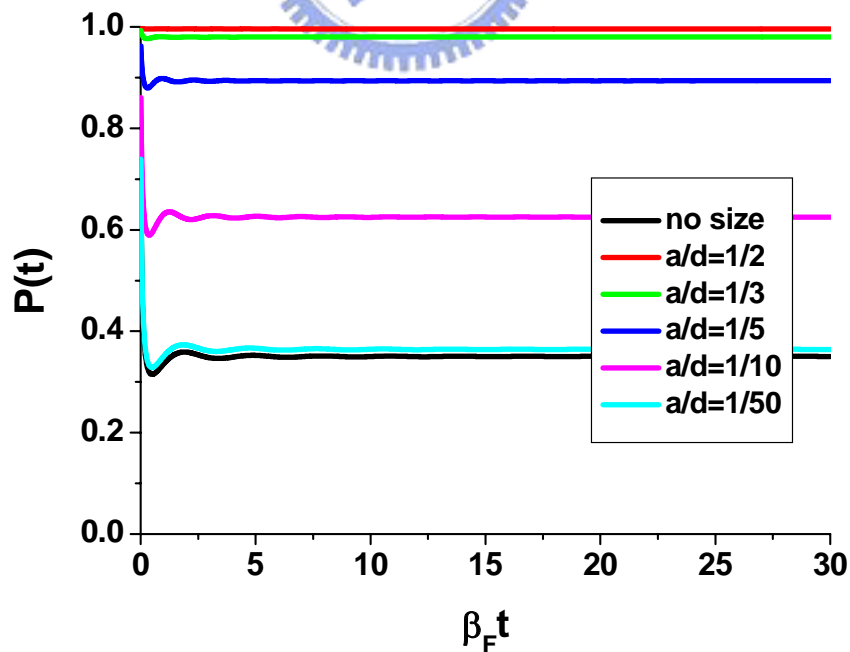


**Fig. 3-7.** Atomic population on the excited atomic state, as a function of  $\beta_F t$ , for  $\Delta/\omega_F = -5$  with various values of ratio from  $a/d = 1/2$  (red line) to  $a/d = 1/10$  (magenta line) and without the finite-size effect (black line).

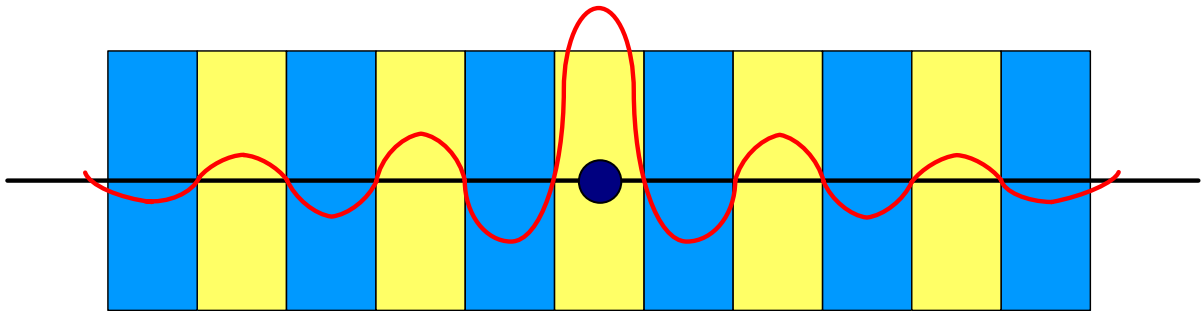


**Fig. 3-8.** Schematic illustration of the enlarging electric field distribution associated with an atom in photonic crystal.

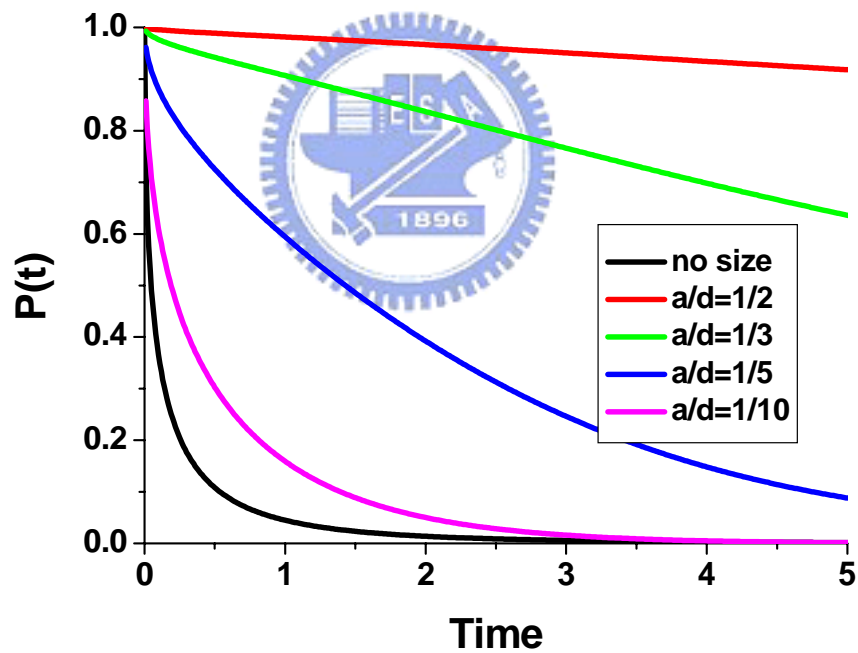


**Fig. 3-9.** Atomic population on the excited atomic state, as a function of  $\beta_F t$ , for  $\Delta/\beta_F = 1$  with various values of ratio from  $a/d = 1/2$  (red line) to  $a/d = 1/10$  (magenta line) and without the finite-size effect (black line).

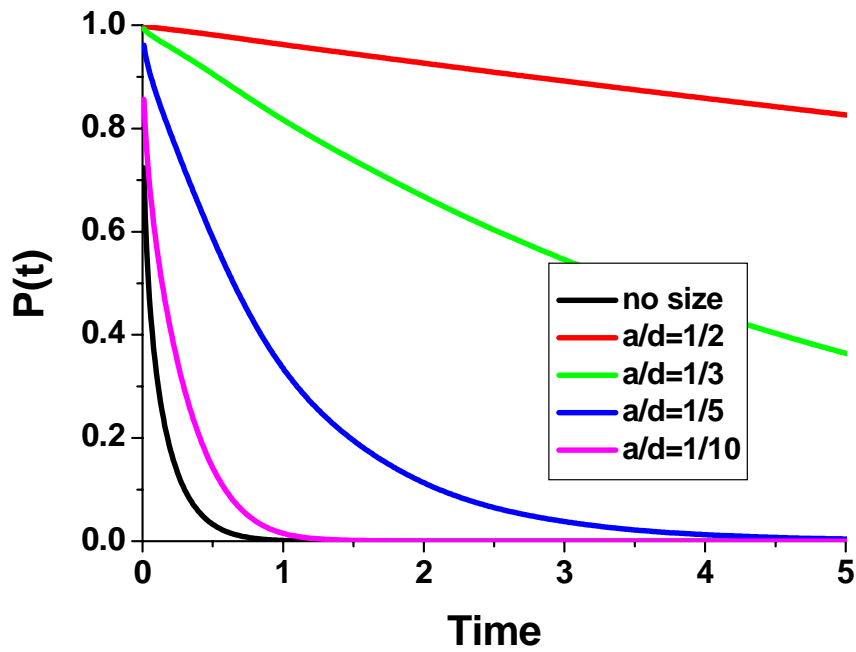


**Fig. 3-10.** Atomic population on the excited atomic state, as a function of  $\beta_F t$ , for  $\Delta/\beta_F = 5$  with various values of ratio from  $a/d = 1/2$  (red line) to  $a/d = 1/10$  (magenta line) and without the finite-size effect (black line).

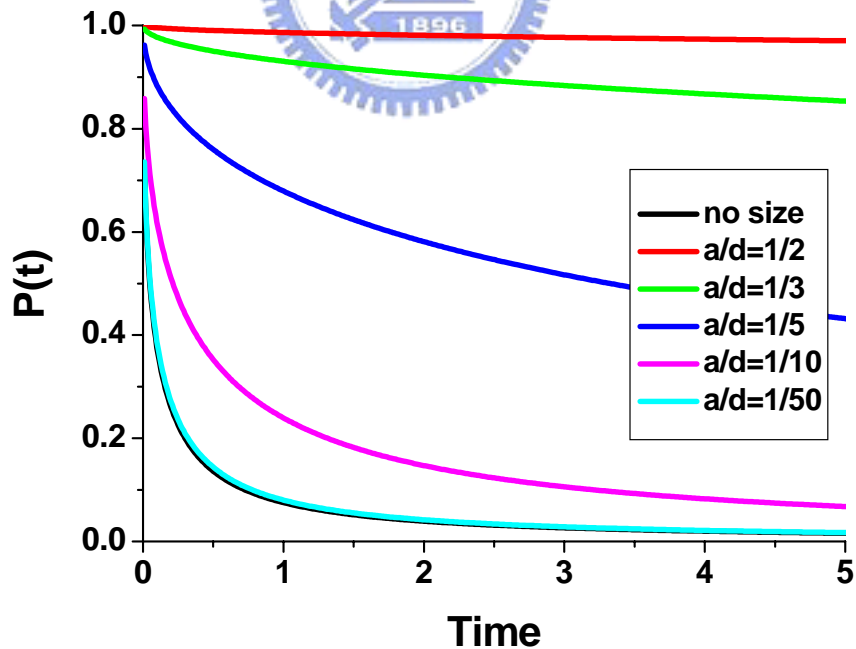


**Fig. 3-11.** Atomic population on the excited atomic state, as a function of  $\beta_F t$ , for  $\Delta/\beta_F = -0.01$  with various values of ratio from  $a/d = 1/2$  (red line) to  $a/d = 1/50$  (cyan line) and without the finite-size effect (black line).

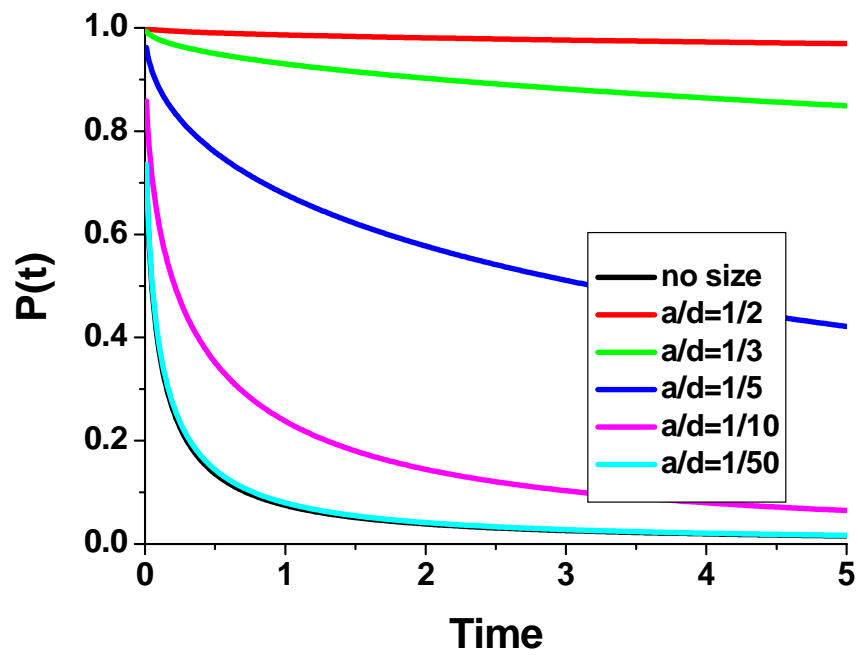
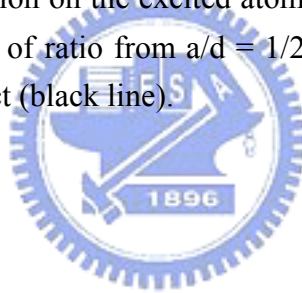


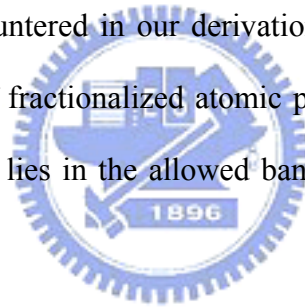
**Fig. 3-12.** Atomic population on the excited atomic state, as a function of  $\beta_F t$ , for  $\Delta/\beta_F = 0.01$  with various values of ratio from  $a/d = 1/2$  (red line) to  $a/d = 1/50$  (cyan line) and without the finite-size effect (black line).



## Chapter 4 Conclusion and Future works

### 4-1 Conclusion

The dynamics of the spontaneous emission of an atom in a photonic crystal can be treated by the fractional calculus. For the first time to our knowledge we show that it is a fractal phenomenon that induces the long-time memory of the spontaneous emission in the photonic crystal. Fractional memory kernel was derived in the long time limit as a result of rapidly varying in frequency near a photonic band edge where the density of electromagnetic modes possesses singularity. We also show that there is no multiple-valued problem encountered in our derivation. Contrary to the previous study, there is no unphysical state of fractionalized atomic population in the excited state when the resonant atomic frequency lies in the allowed band even extremely close to the band edge.



The atomic population on excited state as a function of the scale time for various values of the atomic detuning *outside* the photonic band gap vanishes in the long-time limit for isotropic and anisotropic model. We can see that as  $\Delta_c$  increases, the decay rate very rapidly. When the population *inside* or *at* the band gap, we found the excited-state population exhibits decay and oscillation behavior before reaching a nonzero steady-state value due to photon localization. Besides to near band edge, a superposition of the continuum states and a bound state leads the emitted photon to the atom in anisotropic model.

Finally, we use various values of  $a/d$  to calculate the probability of the atom with finite-size effect. We find that the excited-state population within the band gap exhibits

decay and oscillatory behavior before reaching a nonzero steady-state which is bigger as the atom size increasing. On the other hand, when the atomic detuning in the allowed band, the decay rate decreases as the size increasing. These effects are due to the atom-field coupling that causes field confinement.

## 4-2 Future works

The band structure of photonic crystals is an important factor for spontaneous emission of an atom under atom-field interaction. In our previous studies, the dispersion relation of photonic crystal about the upper band edge (the air band) and only one band were considered. Therefore, we will also consider the lower band (the dielectric band) and multiple bands in the future. The existence of multiple bands in the density of states will allow for a more realistic description of the dynamics.

On the other hand, driving a multi-level atom with a sufficiently strong resonant field alters the radiative dynamics in a fundamental way. It leads to such interesting effects as the enhancement of the index of refraction with greatly reduced absorption, electromagnetically and optical amplification without population inversion. In a three-level atoms are of particular interest in quantum optics and predictably their behavior in the context of structured reservoirs has been addressed. This includes ladder,  $\Lambda$  and V type arrangements. In view of these results, it would be interesting to investigate the combines effects of coherent control by an external driving field and photon localization facilitated by embedded in a photonic band gap material. Hence, our future work is to investigate the coherent control of spontaneous emission for a three-level atom located within in a perfect photonic band gap structure.

Due to the technical difficulties in producing the three-dimension (3D) photonic crystal band-gap materials with a sufficiently large and complete band gap, an unambiguous experimental proof of this effect has, however, not been achieved until now. On the other hand, it is well known that the radiative decay of an atom can be substantially altered by frequently repeated measurements. This result of the interplay between quantum dynamics and measurement, which is absent in classical measurements, is known as the quantum Zeno, (decay suppression) or quantum-anti-Zeno (decay acceleration) effects. Therefore, in the future, we hope to study deeper research for example with quantum measurement and the behavior of an atom in photonic crystal by using Quantum Optics.



## Appendix A. Hamiltonian of a two-level atom interaction with a field [16]

In this appendix we derive the total Hamiltonian from a gauge invariance point of view in semiclassical theory and quantum theory by using dipole approximation. A semiclassical theory of the interaction of a single two-level atom with a single mode of the field in which the atom is treated as a quantum two-level system and the field is treated classically. Otherwise, we also treat the atom-field interaction Hamiltonian in fully quantum theory where a quantized description of the field is required.

### A-1 Local gauge invariance and minimal-coupling Hamiltonian

The motion of a free electron is described by the Schrödinger equation


$$\frac{-\hbar^2}{2m} \nabla^2 \psi = i\hbar \frac{\partial \psi}{\partial t}, \quad (\text{A.1})$$

such that  $P(\vec{r}, t) = |\psi(\vec{r}, t)|^2$  gives the probability density of finding an electron at position  $\mathbf{r}$  and time  $t$ . In Eq. (A.1), if  $\psi(\vec{r}, t)$  is a solution so is  $\psi_1(\vec{r}, t) = \psi(\vec{r}, t) \exp(i\chi)$  where  $\chi$  is an arbitrary constant phase. The probability density  $P(\vec{r}, t)$  would also remain unaffected by an arbitrary choice of  $\chi$ . Thus the choice of the phase of the wave function  $\psi(\vec{r}, t)$  is completely arbitrary, and two functions differing only by a constant phase factor represent the same physical state.

The situation is different, however, if the phase is allowed to vary *locally*, i.e. to be a function of space and time variables as

$$\psi(\vec{r}, t) \rightarrow \psi(\vec{r}, t) e^{i\chi(\vec{r}, t)}. \quad (\text{A.2})$$



The probability  $P(\vec{r}, t)$  remains unaffected by this transformation, but the Schrödinger equation (A.1) is no longer satisfied. We examine the problem of an electron bound by a potential  $V(r)$  which arises from the electrostatic potential that binds the electron to the nucleus and want to satisfy *local* gauge (phase) invariance, then the Schrödinger equation must be modified by adding new terms to Eq. (A.1)

$$\left\{ \frac{-\hbar^2}{2m} [\nabla - i \frac{e}{\hbar} A(\vec{r}, t)]^2 + eU(\vec{r}, t) + eV(\vec{r}) \right\} \psi = i\hbar \frac{\partial \psi}{\partial t}, \quad (\text{A.3})$$

where  $A(\vec{r}, t)$  and  $U(\vec{r}, t)$  are vector and scalar potentials of the electromagnetic field, respectively, which must be inserted into Eq. (A.1) if we want to be able to make the transformation Eq. (A.2), and are given by

$$A(\vec{r}, t) \rightarrow A(\vec{r}, t) + \frac{\hbar}{e} \nabla \chi(\vec{r}, t), \quad (\text{A.4})$$

$$U(\vec{r}, t) \rightarrow U(\vec{r}, t) - \frac{\hbar}{e} \frac{\partial}{\partial t} \chi(\vec{r}, t), \quad (\text{A.5})$$

The gauge-independent quantities are the electric and magnetic fields

$$\vec{E} = -\nabla U - \frac{\partial \vec{A}}{\partial t}, \quad (\text{A.6})$$

$$\vec{B} = \nabla \times \vec{A}. \quad (\text{A.7})$$

Equation (A.3), which is the logical extension of Eq. (A.1) due to the requirement of local gauge (phase) invariance, has the form

$$H \psi = i\hbar \frac{\partial \psi}{\partial t}, \quad (\text{A.8})$$

where  $H$  being the minimal-coupling Hamiltonian.

The minimal-coupling Hamiltonian for an interaction between an atom and the

radiation field can be reduced to a simple form by using the *dipole approximation*. Consider an atom interacting with a radiation field represented by a vector potential  $\mathbf{A}(\mathbf{r}_0 + \mathbf{r}, t)$ . This vector potential may be written in the dipole approximation,  $\mathbf{k} \cdot \mathbf{r} \ll 1$ , as

$$\begin{aligned}\mathbf{A}(\mathbf{r}_0 + \mathbf{r}, t) &= \mathbf{A}(t) \exp[i\mathbf{k} \cdot (\mathbf{r}_0 + \mathbf{r})] \\ &= \mathbf{A}(t) \exp(i\mathbf{k} \cdot \mathbf{r}_0)(1 + i\mathbf{k} \cdot \mathbf{r} + \dots) \\ &\approx \mathbf{A}(t) \exp(i\mathbf{k} \cdot \mathbf{r}_0).\end{aligned}\tag{A.9}$$

The Schrödinger equation in the dipole approximation with  $\mathbf{A}(\mathbf{r}, t) = \mathbf{A}(\mathbf{r}_0, t)$  is given by Eq. (A.3), i.e.,

$$\left\{ \frac{-\hbar^2}{2m} [\nabla - i\frac{e}{\hbar} A(\vec{r}_0, t)]^2 + eV(\vec{r}) \right\} \psi(\vec{r}, t) = i\hbar \frac{\partial \psi(\vec{r}, t)}{\partial t},\tag{A.10}$$

which are working in the radiation gauge, in which  $U(\vec{r}, t) = 0$  and  $\nabla \cdot A = 0$ . Therefore the total Hamiltonian can be obtained as

$$H_{\text{tot}} = \frac{-\hbar^2}{2m} [\nabla - i\frac{e}{\hbar} A(\vec{r}_0, t)]^2 + eV(\vec{r}).\tag{A.11}$$

## A-2 $\mathbf{r} \cdot \mathbf{E}$ Hamiltonian

We proceed to simplify Eq. (A.10) by defining a new wave function  $\phi(\mathbf{r}, t)$  as

$$\psi(\vec{r}, t) = \exp\left[\frac{ie}{\hbar} A(\vec{r}_0, t) \cdot \vec{r}\right] \phi(\vec{r}, t)\tag{A.12}$$

by applying the gauge transformation

$$\chi(\vec{r}, t) = -eA(\vec{r}_0, t) \cdot \vec{r} / \hbar.\tag{A.13}$$

Inserting Eq. (A.12) into Eq. (A.10), we find

$$i\hbar \left[ \frac{ie}{\hbar} \dot{\mathbf{A}} \cdot \vec{r} \phi(\vec{r}, t) + \dot{\phi}(\vec{r}, t) \right] = \left[ \frac{p^2}{2m} + eV(\vec{r}) \right] \phi(\vec{r}, t), \quad (\text{A.14})$$

where  $\vec{p} = -i\hbar\nabla$  is the canonical momentum operator. Taking the simple form as

$$i\hbar \dot{\phi}(\vec{r}, t) = \left[ H_A - e\vec{r} \cdot \vec{E}(\vec{r}_0, t) \right] \phi(\vec{r}, t), \quad (\text{A.15})$$

where

$$H_A = \frac{p^2}{2m} + eV(r), \quad (\text{A.16})$$

is the Hamiltonian of the free atom and we use  $\vec{E}(\vec{r}_0, t) = -\dot{\mathbf{A}}$ . Therefore, the total

Hamiltonian is  $H_{\text{tot}} = H_A + H_{\text{int}}$  with

$$H_{\text{int}} = -e\vec{r} \cdot \vec{E}(\vec{r}_0, t). \quad (\text{A.17})$$

which is interaction Hamiltonian in dipole approximation.

### A-3 $\mathbf{p} \cdot \mathbf{A}$ Hamiltonian

The Hamiltonian can be also expressed in terms of the canonical momentum  $\mathbf{p}$  and the vector potential  $\mathbf{A}$ . We again choose a radiation gauge in which  $U(\vec{r}, t) = 0$  and  $\nabla \cdot \mathbf{A} = 0$ . By using the canonical momentum operator  $\vec{p} = -i\hbar\nabla$ , the total Hamiltonian in Eq. (A.11) can be written as

$$H_{\text{tot}} = \frac{1}{2m} \left[ \vec{p} - e\vec{A}(\vec{r}_0, t) \right]^2 + eV(\vec{r}). \quad (\text{A.18})$$

We may write Eq. (A.17) as

$$H_{\text{tot}} = \frac{\vec{p}^2}{2m} + eV(\vec{r}) - \frac{e}{m} \vec{A}(\vec{r}_0, t) \cdot \vec{p} + \frac{e^2}{2m} \vec{A}^2(\vec{r}_0, t). \quad (\text{A.19})$$

Therefore, the total Hamiltonian  $H_{\text{tot}} = H_A + H_{\text{int}}$  where  $H_A$  is given by Eq. (A.16) and

$$H_{\text{int}} = -\frac{e}{m} \vec{A}(\vec{r}_0, t) \cdot \vec{p} + \frac{e^2}{2m} \vec{A}^2(\vec{r}_0, t). \quad (\text{A.20})$$

is the interaction Hamiltonian. In Eq. (A.20), the first term of represents the interaction between the electron momentum  $\mathbf{p}$  and the radiation field  $\mathbf{A}$  and the second term represents the energy of mutual interaction between radiation fields through the coupling of the electron to the field. The second term in eq. (A.20) is usually small and can be ignored. Hence, the total Hamiltonian is  $H_{\text{tot}} = H_A + H_{\text{int}}$  with

$$H_{\text{int}} = -\frac{e}{m} \vec{A}(\vec{r}_0, t) \cdot \vec{p}. \quad (\text{A.21})$$



#### **A-4 Fully quantum theory**

In the preceding sections concerning the interaction of a radiation field with matter, we assumed the field to be classical. In many situations this assumption is valid. There are, however, many instances where a classical field fails to explain experimentally observed results and a quantized description of the field is required.

Due to the quantum aspects of the field, the total Hamiltonian is treated by adding the energy of the quantized radiation field  $H_F$ . Therefore, the  $\mathbf{r} \cdot \mathbf{E}$  and the  $\mathbf{p} \cdot \mathbf{A}$  interaction Hamiltonian respectively as

$$H_{\text{tot}} = H_A - e\vec{r} \cdot \vec{E}(\vec{r}_0, t) + H_F, \quad (\text{A.22})$$

and

$$H_{\text{tot}} = H_A - \frac{e}{m} \vec{A}(\vec{r}_0, t) \cdot \vec{p} + H_F, \quad (\text{A.23})$$

where  $H_A$  is the Hamiltonian of the free atom in Eq. (A.16).



## Reference

- [1] D. Kleppner, **Phys. Rev. Lett.** **47**, 233 (1981)
- [2] Y. Yamamoto and R. E. Slusher, **Phys. Today** **46(6)**, 66 (1993)
- [3] E. Yablonovitch, T.J. Gmitter, and K.M. Leung, **Phys. Rev. Lett.** **67**, 2295 (1991)
- [4] E. Yablonovitch, **Phys. Rev. Lett.** **58**, 2059 (1987)
- [5] S. John, **Phys. Rev. Lett.** **58**, 2486 (1987)
- [6] S. John and J. Wang, **Phys. Rev. Lett.** **64**, 2418 (1990) and **Phys. Rev. B** **43**, 12772 (1991)
- [7] N. Vats and S. John, **Phys. Rev. A** **58**, 4168 (1998)
- [8] P. Meystre and M. Sargent, *Elements of Quantum Optics* (Springer-Verlag, New York, 1991)
- [9] W. H. Louisell, *Quantum Statistical Properties of Radiation* (Wiley, New York, 1973)
- [10] R. F. Nabiev, P. Yeh, and J. J. Sanchez Mondragon, **Phys. Rev. A** **47**, 3380 (1993)
- [11] S. John and T. Quang, **Phys. Rev. A** **50**, 1764 (1994)
- [12] A. G. Kofman, G. Kurizki and B. Sherman, **J. Mod. Opt.** **41**, 353 (1994)
- [13] C.-q Cao, W. Long and J. Wei, **Phys. Rev. A**, **64**, 043810 (2001)
- [14] V. Weisskopf and E. Wigner, **Z. Phys.** **63**, 54 (1930)
- [15] W. Meissbluth, *Photon-Atom Interactions* (Academic Press, San Diego, 1989)
- [16] M. O. Scully and M. S. Zubairy, *Quantum Optics* (Cambridge University Press, Cambridge, 1997)
- [17] D. G. Angelakis, E. Paspalakis and P. L. Knight, **Phys. Rev. A** **64**, 013801 (2001)
- [18] I. S. Gradshteyn and I. M. Ryzhik, *Table of Integrals, Series and Products* (Academoc Press, New York, 1980)

- [19] K. S. Miller and B. Ross, *An Introduction to the Fractional Calculus and Fractional Differential Equations* (John Wiley & Sons, Inc., New York, 1993)
- [20] I. Podlubny, *Fractional Differential Equations* (Academic, San Diego, 1999)
- [21] M. Floreseu and S. John, **Phys. Rev. A** **69**, 053810 (2004)
- [22] C. Kittel, *Introduction to Solid State Physics* (Wiley, New York, 1980)
- [23] S. John and J. Wang, **Phys. Rev. B** **43**, 12772 (1991)
- [24] J. D. Joannopoulos, *Photonic crystals. Molding the Flow of Light* (Princeton University Press, Princeton, 1995)

